AD-A047 195 RENSSELAER POLYTECHNIC INST TROY N Y F/G 13/5
PREVENTION OF HYDROGEN-INDUCED CRACKING IN HY-130 WELDMENTS.(U)
SEP 77 W F SAVAGE, E F NIPPES, A J SILVIA N00014-75-C-0944

UNCLASSIFIED NL

1 OF 1
AD A047195

END
DATE FILMED
1-78
DDC

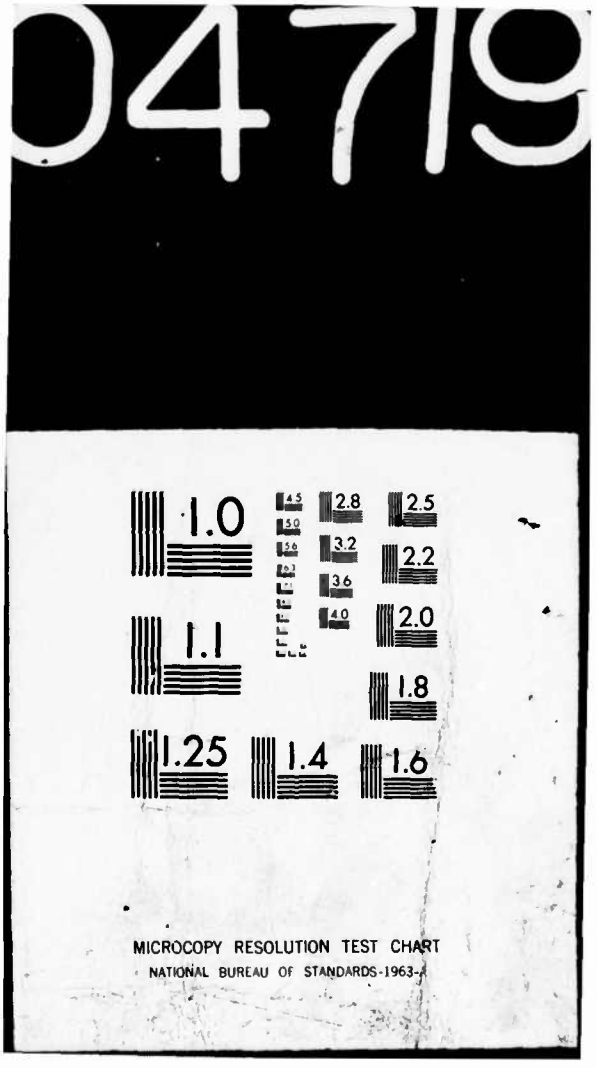
04719
1.0
1.1
1.25
1.4
1.6
1.8
2.0
2.2
2.5
2.8
3.2
3.6
4.0
4.5
5.0
MICROCOPY RESOLUTION TEST CHART
NATIONAL BUREAU OF STANDARDS-1963-A

12

B.S.

OFFICE OF NAVAL RESEARCH
CONTRACT NO. N00014-75-C-0944, NR 031-780

INTERIM
TECHNICAL REPORT
for the period
July 1, 1976 to June 30, 1977

"PREVENTION OF HYDROGEN-INDUCED CRACKING IN HY-130 WELDMENTS"

by

W. F. Savage, E. F. Nippes, and A. J. Silvia

OFFICE OF NAVAL RESEARCH
CONTRACT NO. N00014-75-C-0944 NR 031-780

(15)

(9) INTERIM TECHNICAL REPORT, 1 Jul 76-30 Jun 77,
for the period
July 1, 1976 to June 30, 1977

(6) "PREVENTION OF HYDROGEN-INDUCED CRACKING IN HY-130 WELDMENTS"

by

(10) W. F. Savage, E. F. Nippes, A. J. Silvia

(11) 30 Sep 77

(12) 60 p.

Rensselaer Polytechnic Institute
Troy, N. Y. 12181

302 100

TABLE OF CONTENTS

LIST OF TABLES

LIST OF FIGURES

LIST OF FIGURES - Cont'd.

ACKNOWLEDGMENTS

The work performed under this contract was supported by the Office of Naval Research, Metallurgy Program, which is under the direction of Mr. P. A. Clarkin. Technical monitoring of the program was provided by Dr. Bruce A. MacDonald. The authors greatly appreciate this financial and technical support.

The contractual administrative support, supplied by Mr. Willard Fostel, Administrative Contracting Officer (ONR, New York), is appreciatively acknowledged.

The authors are indebted to Thomas V. Natale and Doreen J. Ball, who participated in the research effort.

ABSTRACT

The investigation was centered on the effect of preheat and postheat treatments on the hydrogen content and initiation and propagation of hydrogen-induced cracks in HY-130 weldments. The initiation and propagation of cracks in welds deposited using both the GMA and SMA processes were studied by the augmented strain cracking test (ASC test). The weld metal hydrogen contents for the various weld beads were determined by the BWRA/IIW technique.

Cracking was found to depend on the base material, augmented strain, hydrogen content, and weld energy input used, but the relationships among these variables are complex. The measured hydrogen contents of the deposited welds were found to depend on the weld energy input, the bead size, and the preheat and postheat treatments.

It was found that hydrogen-induced cracking was nucleated predominately along grain boundaries within the weld metal. However, some cracking was observed to be associated with elongated nonmetallic inclusions in the partially melted zone and the true heat-affected zone.

INTRODUCTION AND HISTORICAL REVIEW

Since World War II, the demand for high-performance steels in the construction of long-span bridges, buildings, pressure vessels, and submarines has led to the development of a new series of quenched-and-tempered, high-strength, low-carbon, low-alloy steels. These new steels, known as the HY steels, exhibit the excellent strength, fracture toughness, corrosion resistance and weldability required for heavy structural applications. Unfortunately as the yield strength is increased, steels become increasingly sensitive to hydrogen-induced cracking.

The ability of hydrogen to cause cracking in the weldments of hardenable steels is well known. Hydrogen cracking may occur in either the heat-affected zone or weld metal if four conditions are present simultaneously. These conditions have been defined as: [1]

1. A critical concentration of diffusible hydrogen at a crack tip,
2. A stress intensity of significant magnitude,
3. A susceptible microstructure, and
4. A temperature in the range of -150 to 400°F (-101 to 204°C).

In welded HY-steel structures, the combination of service and residual stresses, ambient service temperatures, and susceptible microstructures is inevitably present. Therefore, strict control of hydrogen content must be maintained to ensure a fail-safe structure.

Hydrogen is introduced into weldments because the welding arc is capable of dissociating hydrogen gas, water vapor, and hydrogen-bearing compounds to produce atomic hydrogen. Furthermore, the molten metal has an occlusive capacity for atomic hydrogen which is proportional to its concentration in the arc atmosphere. The major sources for this hydrogen are moisture in covered electrodes, contamination in bare filler wire, surface contaminates on the base material, and moisture contained in shielding gases.

Efforts to eliminate hydrogen cracking in HY-80 by controlling the moisture content in bare filler wire have not been totally successful. Unfortunately, HY-130 weldments are even more susceptible to hydrogen-induced cracking than HY-80. The specifications for welding consumables for HY-80 call for a maximum level of 0.2% moisture in the coatings of covered electrodes and 6-8 ppm hydrogen in bare filler wires. The more stringent specifications

for HY-130 welding consumables require a maximum level of 0.1% moisture in coatings of electrodes and 3 ppm hydrogen in bare wires.[2] Such requirements for the control of the hydrogen content of arc atmospheres are not easily met in a shipyard environment. It, therefore, has become necessary to study other procedures for eliminating hydrogen-induced cracking.

Presently two procedures have been proposed to control hydrogen-induced cracking in HY-130 weldments. One procedure attempts to render the weld-metal hydrogen innocuous by chemical combination to form a hydride. Rare earths can be added to the filler metal to form hydrides. Unfortunately, such additions have been shown to make the manufacturing of filler wire more difficult, and could possibly be detrimental to the mechanical properties of HY-130.[3]

A second procedure utilizes a low-temperature interpass heat treatment. By maintaining the weld at an elevated temperature, hydrogen can escape rapidly from the weld bead until the hydrogen level falls below that required for cracking. This technique has been used successfully in practice for various steels. However, the level to which hydrogen must drop, and consequently the times for which a weld bead must be held at temperature, have largely been a matter of conjecture.

Delong[4] has recommended a minimum postheat time of one hour and a temperature of 275°F (135°C) for welds made with E14018 electrode. Graville[5] has suggested a minimum time of 1/2 hour for postheats above 250°C (482°F) and increasing times with lower temperature postheats. As might be expected, both postheat time and temperature are dependent upon weld bead thickness.[6] Presently specifications for the fabrication of HY-80 recommend a preheat and postheat treatment of 200°F (93°C) (minimum) to 300°F (149°C) (maximum).[7] Such heat treatments are both cumbersome and expensive.

Although the conditions necessary for hydrogen-induced cracking are well known, there exists considerable controversy over the mechanism of hydrogen cracking. Four basic theories have been proposed to explain this phenomenon.

Planar-Pressure Theory. The planar-pressure theory was initially proposed by Zapffe and Sime[8] and later modified by Tetleman.[9] Figure 1 shows the variation in solubility of hydrogen with temperature. Note that the solubility falls abruptly from about 25 ppm* in liquid iron to about 6 ppm in body-centered cubic delta ferrite at the melting point (1538°C). The solubility increases from about 4.9 to 8.3 ppm when delta ferrite transforms to

---

* The H concentration in cm^3 per 100 grams of iron is equal to the H concentration in ppm multiplied by 1.12

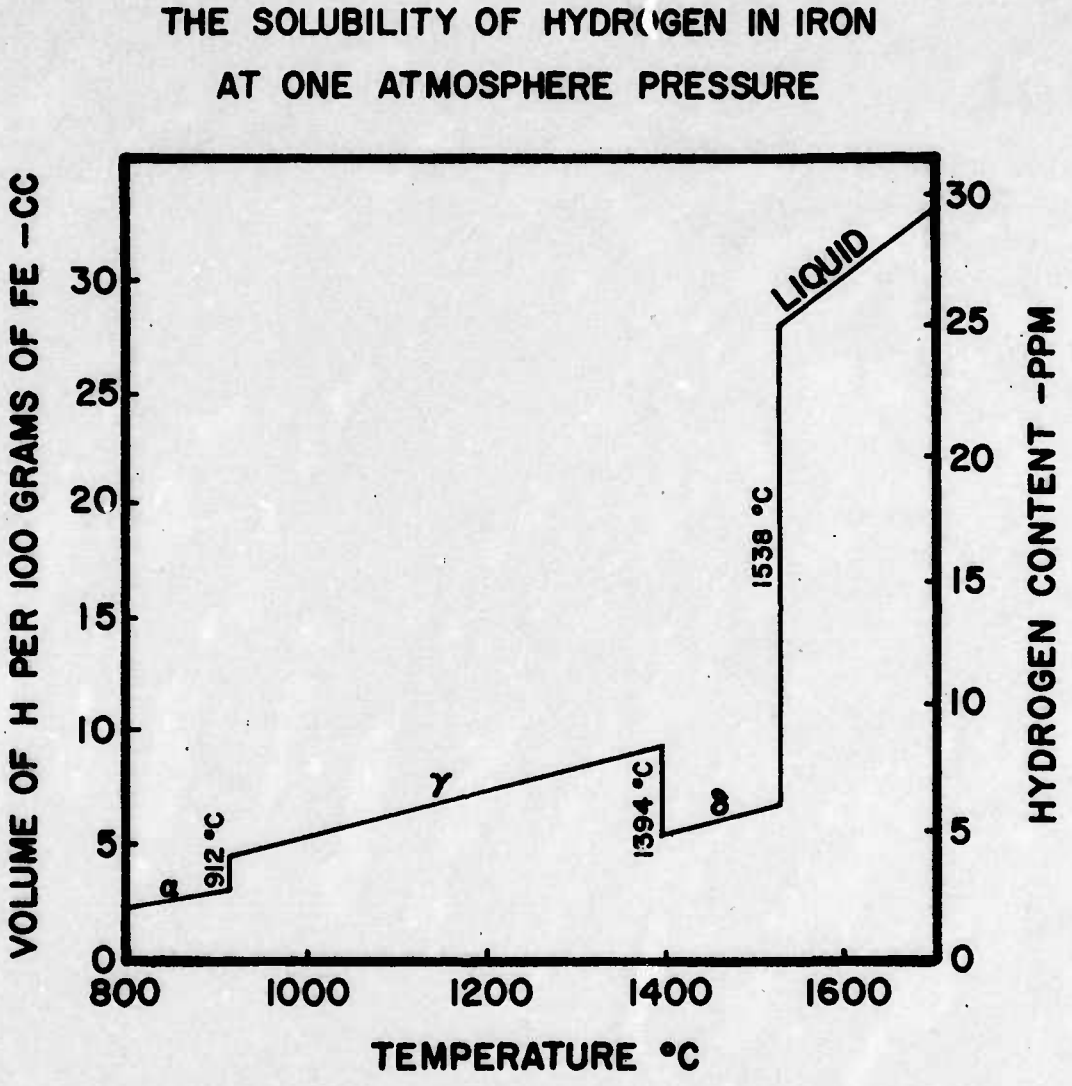
THE SOLUBILITY OF HYDROGEN IN IRON
AT ONE ATMOSPHERE PRESSURE
VOLUME OF H PER 100 GRAMS OF FE -CC
HYDROGEN CONTENT -PPM
TEMPERATURE °C
LIQUID
1538 °C
1394 °C
912 °C
α
γ
δ
0
5
10
15
20
25
30
800
1000
1200
1400
1600

Figure 1

face-centered cubic austenite at 1394°C. The solubility in austenite decreases continuously to about 4.1 ppm at 9.2°C and then drops to 2.7 ppm when the austenite transforms to ferrite at 912°C. The solubility in ferrite then decreases to less than 0.5 ppm at ambient temperature.

This theory postulates that atomic hydrogen diffuses through the iron lattice and precipitates in voids or other defects. Inside these voids, atomic hydrogen reassociates to form molecular hydrogen and thus creates an extremely high internal pressure. The interaction of the high internal pressure with applied and residual stresses is postulated to result in crack initiation and propagation from the initial defect sites.

Surface-Absorption Theory. The surface-absorption theory was initially proposed by Petch[10] and recently modified by Williams and Nelson.[11] This theory postulates that hydrogen absorbed on the surface of internal cracks lowers the surface-free energy and thus reduces the critical fracture stress. Thus, the initial crack is formed by dislocation pileups at a grain boundary, and hydrogen is postulated to influence crack propagation, but to have no effect on crack initiation.

Both these theories have been criticized on the basis of the fact that the incubation time for crack initiation is reversible with respect to the applied stress. Furthermore, the embrittlement persists at very low temperatures where both the bulk diffusion rate and the rate of redistribution of hydrogen along newly created surfaces would be negligibly small.[12]

Triaxial-Stress Theory. Troiano[13] has advanced a triaxial-stress theory which assumes that hydrogen in solution near a void causes embrittlement. This theory predicts that the concentration of hydrogen in the region of maximum triaxial stress near a void or stress raiser, exceeds that in the lattice at equilibrium. It is assumed that hydrogen in the void itself is non-damaging and, that a critical stress level must be exceeded to cause a critical or damaging concentration of hydrogen.

According to Troiano, the diffusion of hydrogen into this region is induced by the stress gradient created by the region of triaxial stress. When the hydrogen concentration reaches a critical concentration in the location of the maximum triaxial stress, initiation of a crack occurs. The crack is propagated by the same mechanism after hydrogen diffuses to the triaxial-stress region ahead of the newly located crack tip.

Hydrogen-Dislocation-Interaction Theory. The fourth theory stresses the interaction of hydrogen with moving dislocations. Two opposing hypotheses

of this interaction have been advanced.

Beachem[14] proposed a theory involving microplasticity mechanisms instead of "embrittlement" mechanisms. In this model, the pressure of hydrogen dissolved in the lattice ahead of the crack tip assists microscopic deformation processes. The presence of dissolved hydrogen, then, lowers the applied stress necessary to cause fracture by a dislocation-multiplication mechanism.

Steinman et al[15] and Berstein[16] have suggested that hydrogen in the lattice acts to reduce the energy required to initiate and propagate fracture by reducing dislocation mobility. This is postulated to cause the development of large local strain concentrations, and lead to initiation and propagation of cracks.

OBJECT

This investigation involved a study of the effects of preheat and postheat temperature and time upon the hydrogen content and hydrogen-induced cracking tendencies of HY-130 weldments.

Specifically, the objectives of this investigation were:

1. To evaluate the interrelationship among the mechanical, metallurgical, and chemical factors responsible for hydrogen-induced cracking in HY-130 steel weldments.
2. To determine the effect of preheat and interpass temperatures and times on the level of hydrogen retained.
3. To study, with the aid of acoustic-emission technology and optical microscopy, the mechanisms for nucleation and propagation of hydrogen-induced cracks.

MATERIALS AND PROCEDURE

Two different heats of 2-in. thick HY-130 steel plate were used in this study. The chemical composition and mechanical properties of each heat and filler material used are listed in Tables I and II.

Metallographic examination of the base materials revealed a significant difference between the nonmetallic inclusion morphologies of the two heats. Heat B contained randomly distributed, fine, spherical inclusions with a small quantity of fine, elongated, sulfide inclusions. Inclusions found in Heat A consisted of fine, spherical inclusions, small elongated sulfides, and large, elongated stringers of a duplex, oxide-sulfide nature. In both heats the fine,

TABLE I

CHEMICAL COMPOSITION OF MATERIALS USED IN THIS INVESTIGATION

MATERIAL	CONDITION	C	Mn	P	S	Si	Ni	Cr	Mo	V	Ti	Al
HY-130 (Heat A)	2" Plate	0.11	0.88	0.003	0.003	0.35	4.95	0.53	0.50	0.08	--	--
HY-130 (Heat B)	2" Plate	0.10	0.77	0.005	0.003	0.20	4.92	0.56	0.52	0.06	0.01	0.026
E14018	3/16" Coated Electrodes	0.066	0.96	0.004	0.004	0.37	3.53	0.46	0.78	0.01	--	--
AX-140	0.045" Bare Wire	0.10	1.86	0.005	0.005	0.43	2.05	0.87	0.54	--	0.01	

TABLE II

MECHANICAL PROPERTIES OF MATERIALS USED

MATERIAL	Y.S. (ksi)	T.S. (ksi)	% ELONGATION (2" Gage Length)
HY-130 (Heat A)	134	145	21
HY-130 (Heat B)	136	147	19
E14018 *	141	147	18
AX-140	139	148	21

Note: Weld Metal Properties for 43 kj/in. Heat Input

* Typical values for this material taken from producer's literature

elongated sulfides and large stringers were located in the steel plate near the mid-thickness, as shown in longitudinal sections in Fig. 2.

To investigate the effect of the differing inclusion morphologies on hydrogen cracking, test specimens were cut from each 2-in. thick plate, as illustrated in Fig. 3. With this orientation, the location of each deposited weld bead corresponded to the mid-thickness of the as-received steel plates.

Specimens were machined to dimensions of 2- x 0.5- x t-inches. Thicknesses, t, of 0.1, 0.2, and 0.3 in. were chosen corresponding to strains of 0.25, 0.50, and 0.75% in the augmented strain cracking (ASC) test. (This test is described later in this section.)

The 2- x 1/2-in. surfaces of each specimen were lapped parallel and flat with 600-grit silicon-carbide paper. The polished specimens were clamped in a welding fixture together with starting and run-off tabs, and 1- x 0.5- x 0.2-in. samples for diffusible hydrogen analysis, as shown in Fig. 4.

Preheating was performed by placing the welding fixture with clamped specimens in a 300°F (149°C) holding oven. After reaching temperature, the fixture was removed from the oven and a weld bead deposited using the desired process and procedures. Shielded metal arc (SMA) welds were deposited using 3/16-in. diameter E14018 electrodes with an automatic stickfeeder. (Fig. 5). The hydrogen level was varied by reconditioning moisture-contaminated electrodes by baking. Gas metal arc (GMA) welds were deposited using AX-140 filler wire. The hydrogen level for GMA was varied by adding controlled amounts of hydrogen to the shielding gas. The welding parameters used for both processes are listed in Table III.

Immediately after depositing the weld bead, the specimens were unclamped from the welding fixture and broken apart. The time interval between weld completion and specimen separation was approximately 3 minutes. The separated specimens were then either quenched or placed in a 300°F (149°C) holding oven for postheat treatment. Selected sets of test specimens were postheated at time intervals of 10, 20, and 30 minutes.

After completion of the desired postheat treatment, the specimens were quenched rapidly into an ice-water bath and then transferred swiftly to a dry ice and alcohol bath to minimize loss of diffusible hydrogen.

One face of each test specimen was repolished for visual observation of hydrogen cracking during the ASC test. During repolishing the specimens were repeatedly quenched into the dry ice and alcohol bath to prevent hydrogen loss.

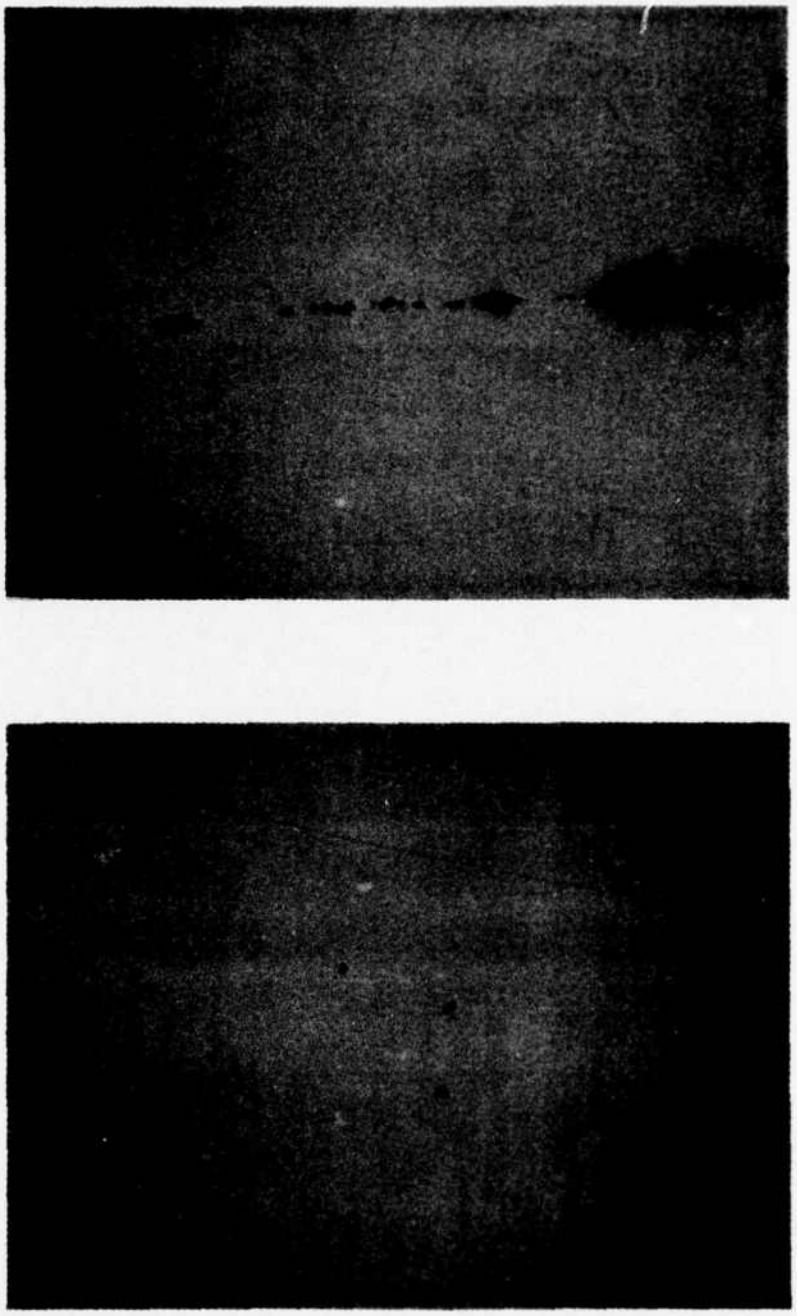

Figure 2

The General Appearance of Non-metallic Inclusions in the Midthickness of the As-received HY-130 Steel Plates. Polished and Unetched, 250X. Top: Heat A, Bottom: Heat B.

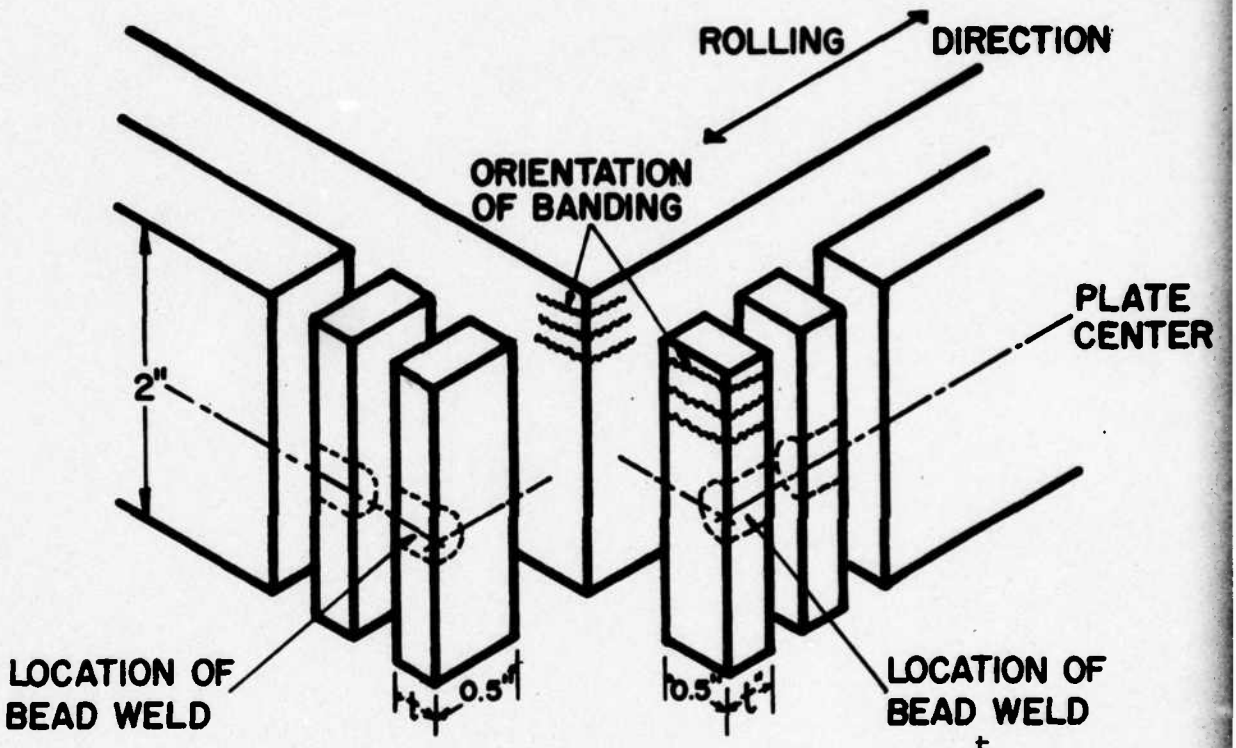

Figure 3

Orientation of the ASC Test Specimens Machined from the As-received HY-130 Steel Plates.

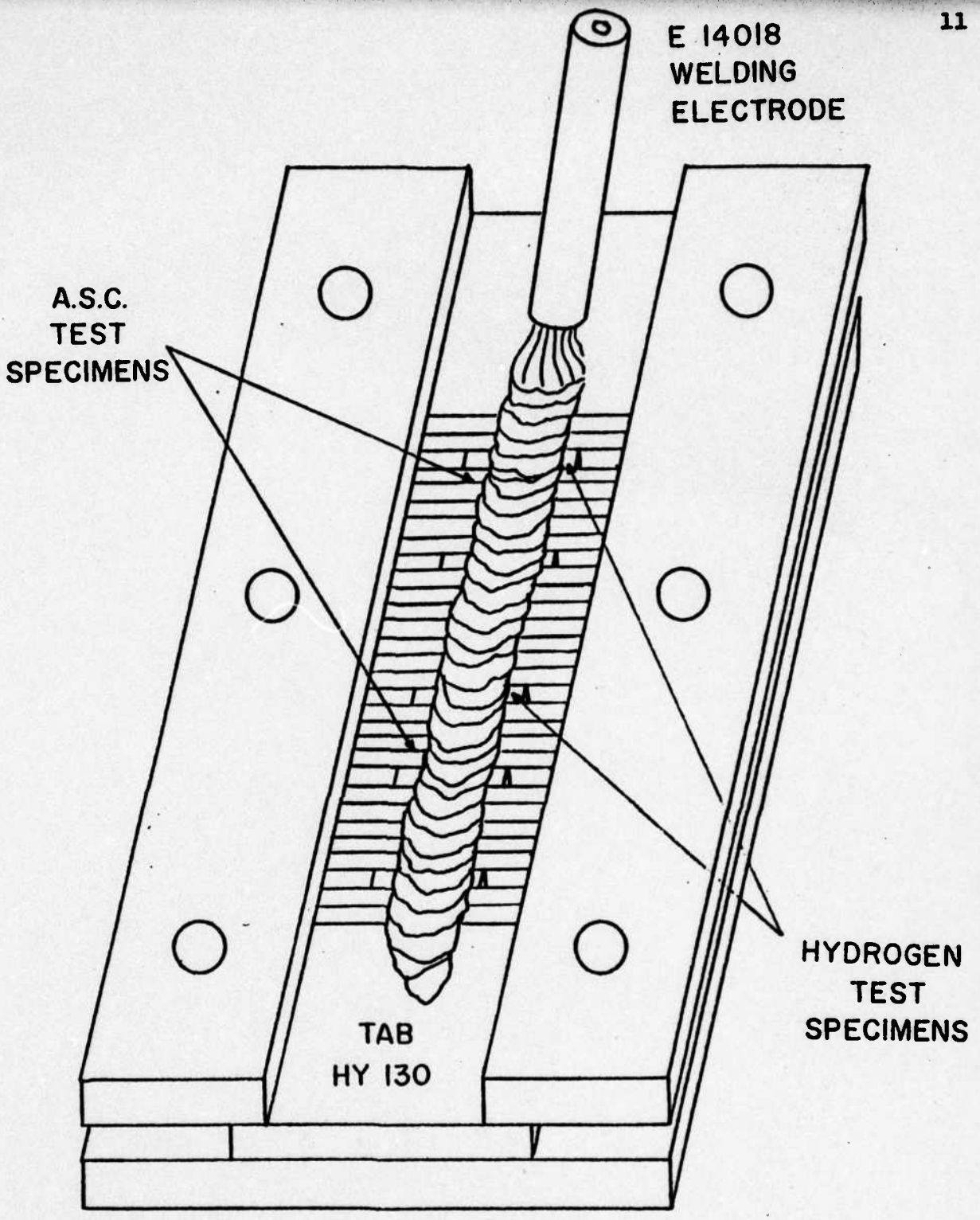

Figure 4

Schematic Illustration Showing the Welding of ASC Test Specimens

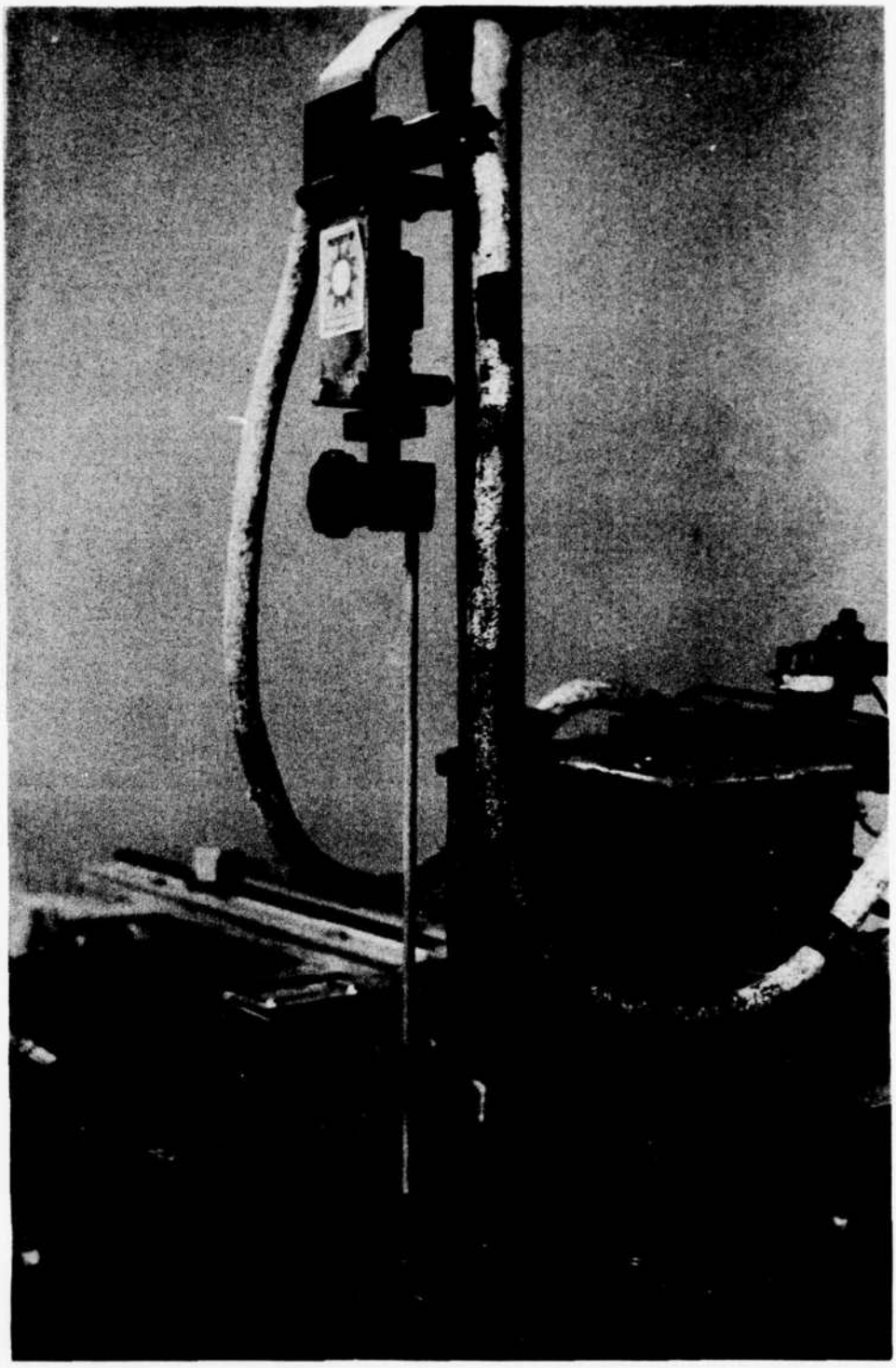

Figure 5

Automatic Stickfeeder Unit for Shielded Metal Arc Welding. Welding Fixture is Directly under the Electrode.

TABLE III

WELDING CONDITIONS USED IN THIS INVESTIGATION

Process	Electrode Diam.(In.)	Voltage (Volts)	Current (Amps)	Travel Speed (Ipm)	Heat Input (Kj/in.)
GMA*	0.045	29-30	200-210	8.7	40
GMA*	0.045	29-30	200-210	11.5r	30
SMA	3/16	23-25	165	5.7	40
SMA	3/16	23-25	165	7.6	30

* Gas Flow 40 CFH of Argon-2% Oxygen and Hydrogen Mixture (See Text)

Augmented Strain Cracking Test (ASC Test). Specimens prepared in the manner described above were stored continuously in liquid nitrogen until testing. They were then mounted in the straining devices shown in Fig. 6. By forcing the specimen to conform to the surface of a radiused die block, a reproducible level of augmented strain is produced at the specimen surface. The approximate value of the augmented strain can be calculated by the relationship:

$$\epsilon = t/2R$$

where

ϵ = augmented strain at the outer surface

t = thickness of the specimen

R = radius of curvature of the die block (normally 20 inches)

After applying the augmented strain in the test fixture, the specimen was was allowed to warm to room temperature and the initiation and growth of hydrogen-induced cracks were both observed under a microscope and monitored acoustically. In this manner the observer was able to study both crack-initiation sites and crack morphologies.

Acoustic-Emission Instrumentation. To provide additional information on the initiation and propagation of hydrogen-induced cracking, the ASC testing device was instrumented to detect acoustic emissions.

The acoustic emissions were monitored using a Model 201 Acoustic Emission Technology Corporation signal processor with a matching preamplifier and accelerometer. (Fig. 7). The processed signals were fed into an X-Y recorder and a plot of total acoustic-emission counts vs. time was obtained. A 125-250 MHZ bandpass filter was used to minimize signals arising from ambient noise in the laboratory. In addition, the testing device was mounted on a padded stand to eliminate any noise from the other test equipment.

The acoustic-emission surveys served two useful purposes. First, the summation of the amplitudes of individual stress-wave emissions have been shown by Hartbower[17] to be directly proportional to the crack extension as measured by a crack-opening-displacement gage. Therefore, a summation of the amplitudes of the stress-wave emissions recorded during testing could be taken as a relative measure of total crack length. Thus, the acoustic-emission data provided information on crack propagation. In addition, the incubation time for crack initiation was obtained from acoustic-emission recordings.

Diffusible-Hydrogen Analysis. The BWRA/IIW technique[18] was employed for determining the amount of diffusible hydrogen in the weld deposits. Five hydrogen-analysis specimens were taken from each weld bead. (Fig. 4). As

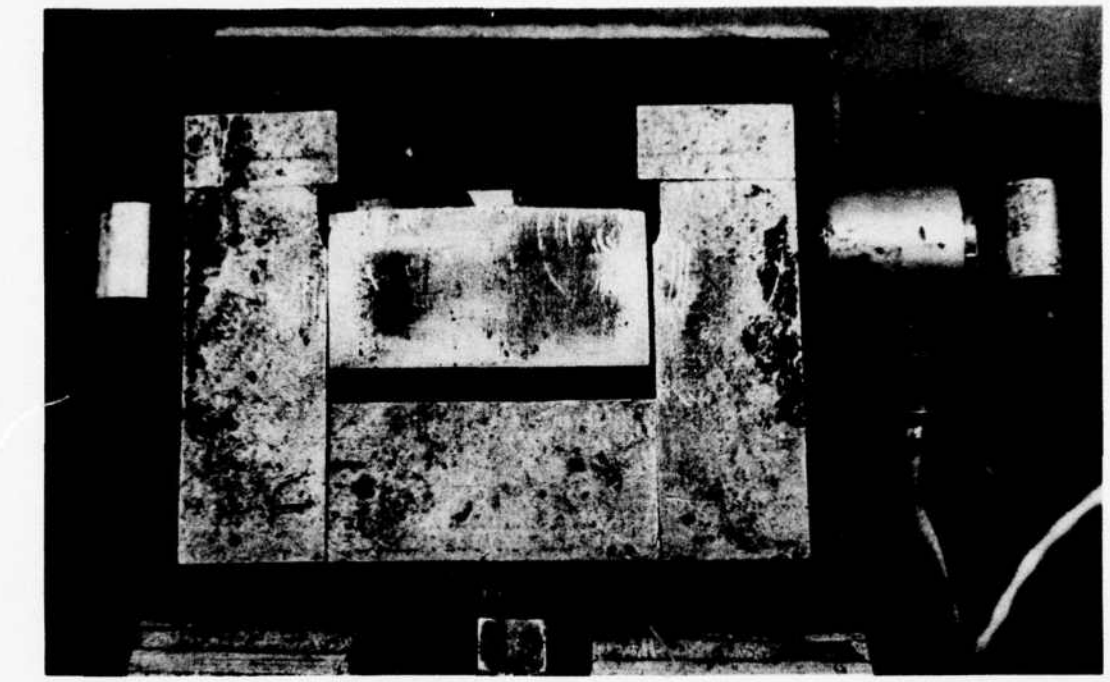

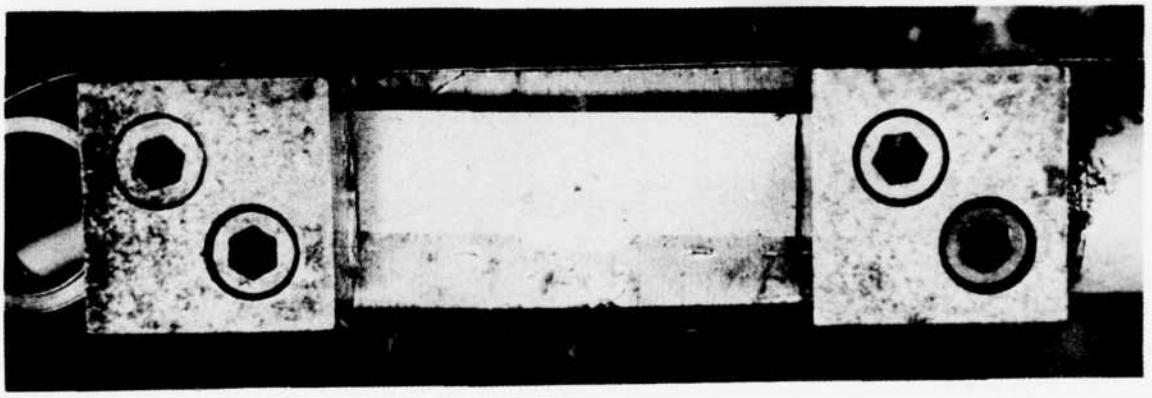

Figure 6

The Augmented Strain Cracking Test Device with Acoustic-Emission Transducer Attached
Top: Overall Side View of the Testing Device.
Bottom: Close-up Top View Showing the Positioning of ASC Test Specimen.

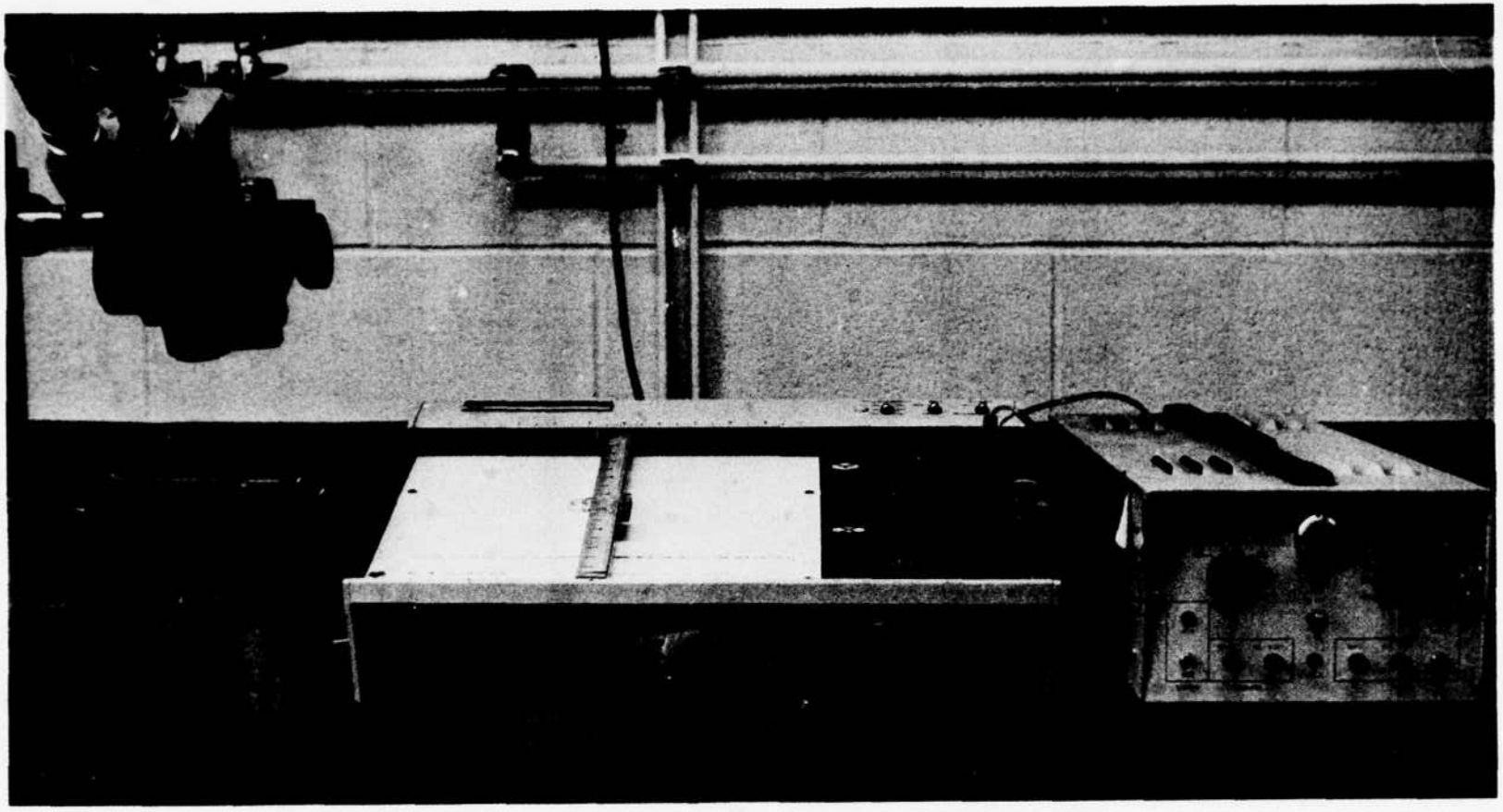

Figure 7

Acoustic-Emission Equipment Set-up with ASC Test Device

with the ASC test specimens, each BWRA/IIW specimen was subjected to a different assigned preheat and/or postheat treatment. In this manner, the effect of preheat and postheat temperature and times on hydrogen content was evaluated.

Metallographic Examination. After 72 hrs. in the ASC test fixture, the specimens were unloaded and prepared for metallographic examination. The different etching procedures employed and their application are listed in Table IV. Photomicrographs were prepared to document the location of crack-initiation sites and the morphology of the hydrogen-induced cracks.

RESULTS AND DISCUSSION

The Role of Augmented Strain

As mentioned previously, the augmented strain in the outer fibers of the ASC test specimens was approximately t/2R. If one assumes an elastic modulus of 30×10^6 psi and an elastic limit of 130 ksi, then the strain at the elastic limit would be 0.43%. This would correspond to a specimen thickness, t, of 0.17 in. for a die with a radius of curvature, R, of 20 in. With this die, the 0.1-in. thick specimens experienced an augmented strain of 0.25%, which corresponds to a calculated elastic maximum fiber stress of 75 ksi. The 0.2-in. and 0.3-in. thick specimens experienced strains of 0.5 and 0.75%, respectively, and were thus subjected to plastic deformation during loading.

It is significant to note that, regardless of the amount of hydrogen, the welding process, the welding energy input, or the preheat and postheat procedures employed, no hydrogen-induced cracking was observed in either heat of HY-130 when subjected to 0.25% augmented strain. However, with both 0.5% and 0.75% augmented strain, various combinations of hydrogen content and welding procedures were found to cause hydrogen-induced cold cracking.

The role of hydrogen content, welding process, energy input, preheat, and postheat procedures will be discussed in detail in the following sections. However, the results of the studies of the role of augmented strain indicate that hydrogen-induced cracking cannot be induced at stress levels significantly below the yield strength of the steel.

The Role of Hydrogen

Preliminary tests suggested that, with yield-strength stress levels, a hydrogen content of less than about 2cc/100 g of added filler metal

TABLE IV

ETCHING PROCEDURES USED IN THIS INVESTIGATION

Procedure	Etchant	Etching Technique	Application
A) Step 1	1% Nital	Immerse for 6-10 sec. and rinse with ethanol only, hot-air dry.	This procedure is excellent for revealing solidification structures, the unmixed zone, and partially melted zone in HY-130 welds.
Step 2	3% Aqueous Sodium Bisulfate with Tridecylbenzene Sulfonate wetting agent	Swab with sodium bisulfate @ 100°F until metal turns dark; then rinse with distilled water and ethanol, then hot-air dry.	
B) Step 1	2% Aqueous Picric Acid with Sodium Tridecylbenzene Sulfonate wetting agent	Temper specimens at 600°C(1112°F) for 1 hour. Etch with solution heated up to about 43°C (110°F).	This procedure is used to reveal solidification structures and the partially melted zone. Etching condition best for revealing prior austenite grain boundaries in HAZ.
Step 2	1% Nital	Immerse for 2-8 sec. and rinse with ethanol only.	

(1.8 ppm*) was required to avoid hydrogen-induced cracking. However, as work progressed, it became evident that the level of diffusible hydrogen measured by the BWRA/IIW technique is dependent upon several factors. Thus, the definition of a universally applicable maximum allowable hydrogen content does not appear possible.

Figures 8 and 9 show the effect of energy input and postheating time at 300°F (149°C) on the diffusible hydrogen content for various initial hydrogen levels.

Figure 8 summarizes the results obtained for GMA welds made with Ar-2% O_2 and mixtures of hydrogen with Ar-2% O_2. With an energy input of 40 kj/in., when no hydrogen was added to the shielding gas, a level of about 1 ppm of diffusible hydrogen was obtained. This hydrogen level was essentially independent of the time the 300°F postheat was applied. The other four plots for GMA welds made with 40 kj/in. show what appears to be an essentially linear decrease in hydrogen content as the postheat at 300°F is increased from 0 to 30 mins. On the other hand, the two plots for welds made with 30 kj/in. show an exponential decrease in diffusible hydrogen content from a significantly higher initial level to about 1 ppm after a 30-min. postheat at 300°F. This apparently anomalous behavior will be explained in the following paragraphs.

Figure 10 shows the effect of energy input and initial plate temperature in SMA welds on the thermal cycles experienced by points in the heat-affected zone where the peak temperature was 2300°F (1260°C).** Attention is drawn to the fact that the cooling portion of the thermal cycle for a weld made with 40 kj/in. without preheat and that for a weld made using 30 kj/in. with 300°F preheat are quite similar down to approximately 750°F (400°C). Furthermore, note that the weld made using 40 kj/in. with a 300°F preheat cools much more slowly, while that made using 30 kj/in. without preheat cools much more rapidly.

From the above, it is obvious that the combination of longer times at higher temperatures, characteristic of the preheated 40 kj/in. welds, allowed a considerable amount of the initial hydrogen to escape before the test sample could be introduced into the BWRA/IIW apparatus. As mentioned previously in Materials and Procedures the time required to remove the specimens from the welding fixture, break them apart, and transfer them

---

* based upon the weight of the filler metal added to the test specimen

** calculated by procedure outlined in Ref. 19

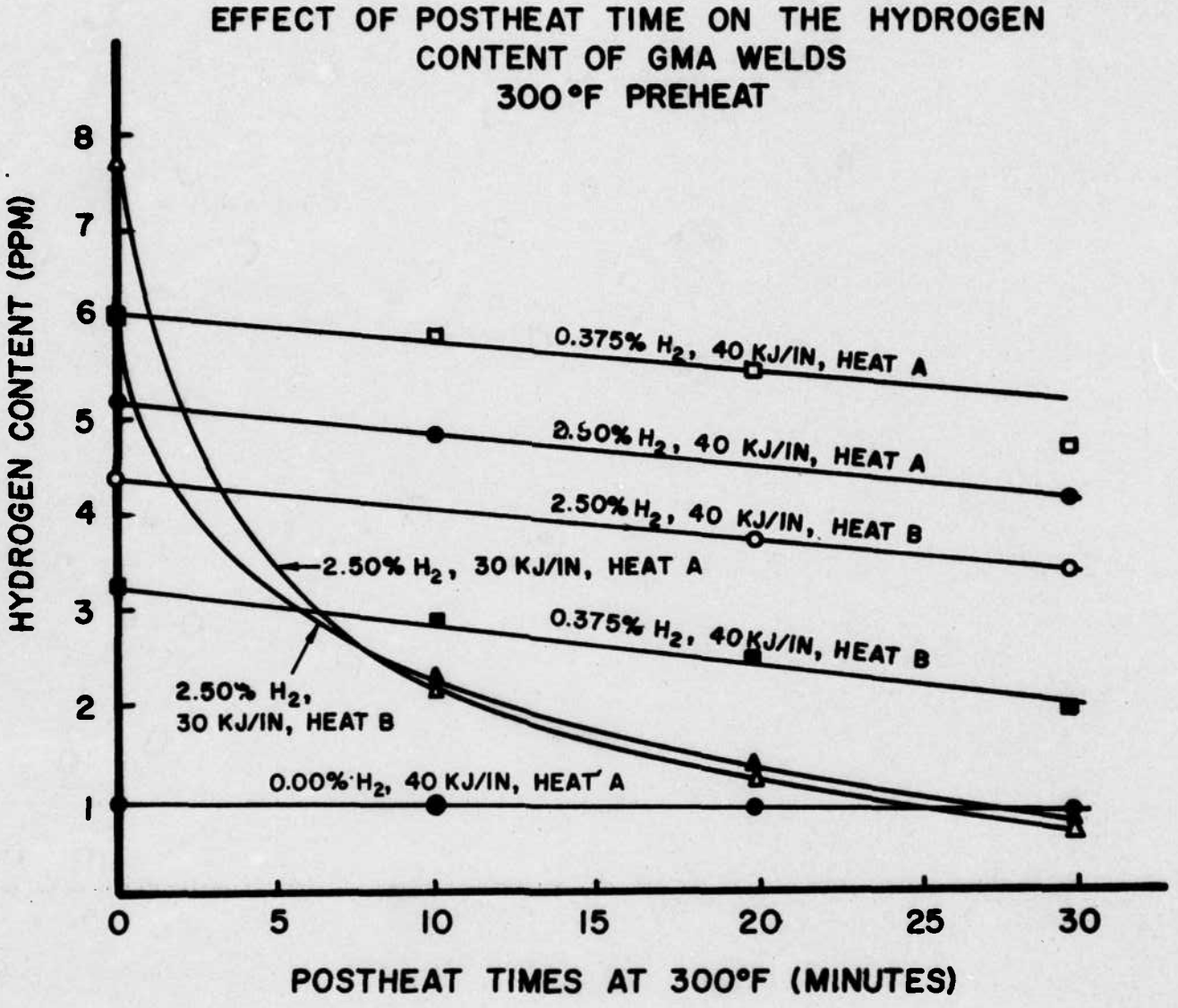
EFFECT OF POSTHEAT TIME ON THE HYDROGEN CONTENT OF GMA WELDS 300°F PREHEAT
HYDROGEN CONTENT (PPM)
8
7
6
5
4
3
2
1
0.375% H2, 40 KJ/IN, HEAT A
2.50% H2, 40 KJ/IN, HEAT A
2.50% H2, 40 KJ/IN, HEAT B
2.50% H2, 30 KJ/IN, HEAT A
0.375% H2, 40 KJ/IN, HEAT B
2.50% H2, 30 KJ/IN, HEAT B
0.00% H2, 40 KJ/IN, HEAT A
0
5
10
15
20
25
30
POSTHEAT TIMES AT 300°F (MINUTES)

Figure 8

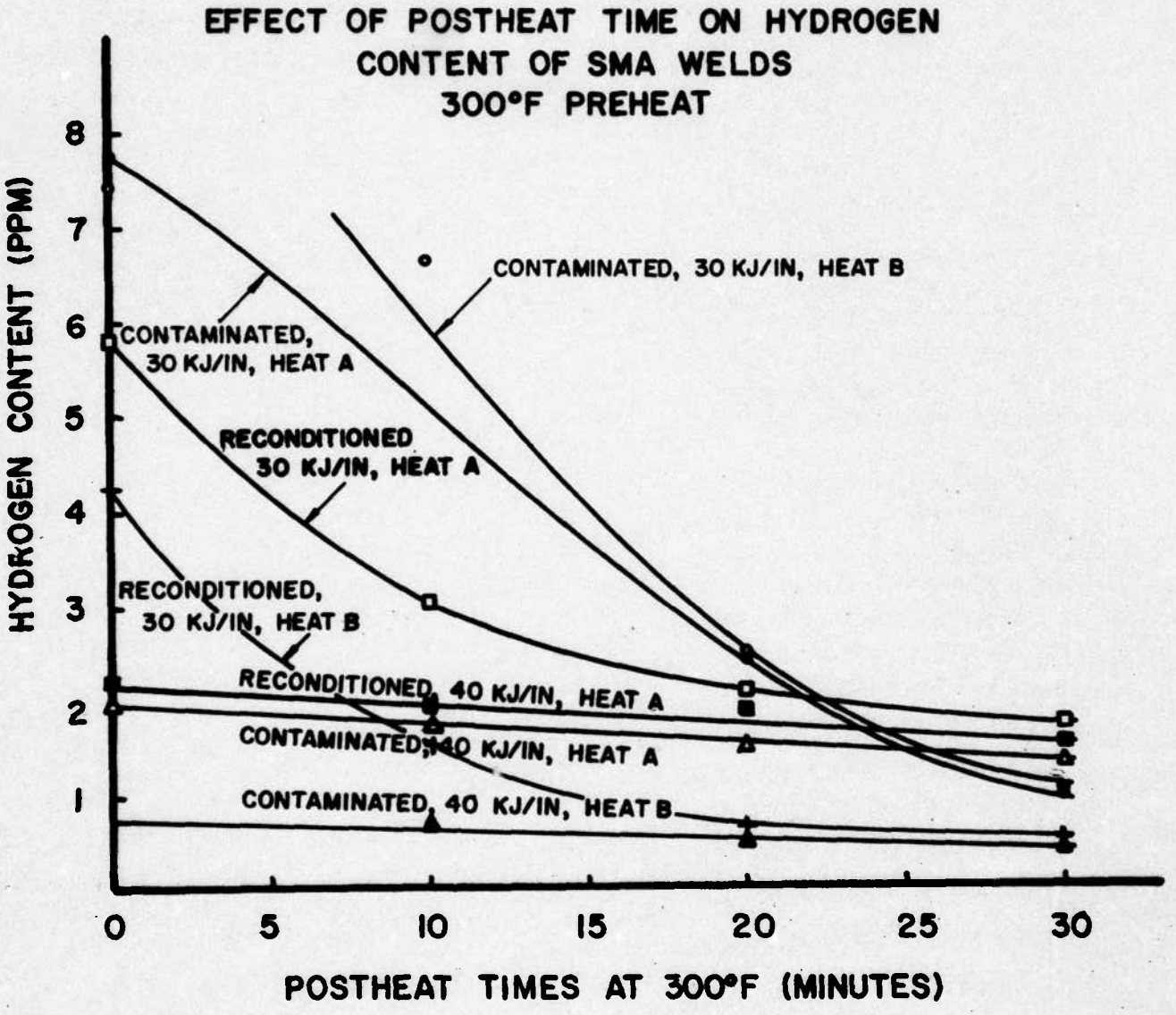
EFFECT OF POSTHEAT TIME ON HYDROGEN CONTENT OF SMA WELDS 300°F PREHEAT
HYDROGEN CONTENT (PPM)
8
7
6
5
4
3
2
1
CONTAMINATED, 30 KJ/IN, HEAT B
CONTAMINATED, 30 KJ/IN, HEAT A
RECONDITIONED 30 KJ/IN, HEAT A
RECONDITIONED, 30 KJ/IN, HEAT B
RECONDITIONED, 40 KJ/IN, HEAT A
CONTAMINATED, 40 KJ/IN, HEAT A
CONTAMINATED, 40 KJ/IN, HEAT B
0
5
10
15
20
25
30
POSTHEAT TIMES AT 300°F (MINUTES)

Figure 9

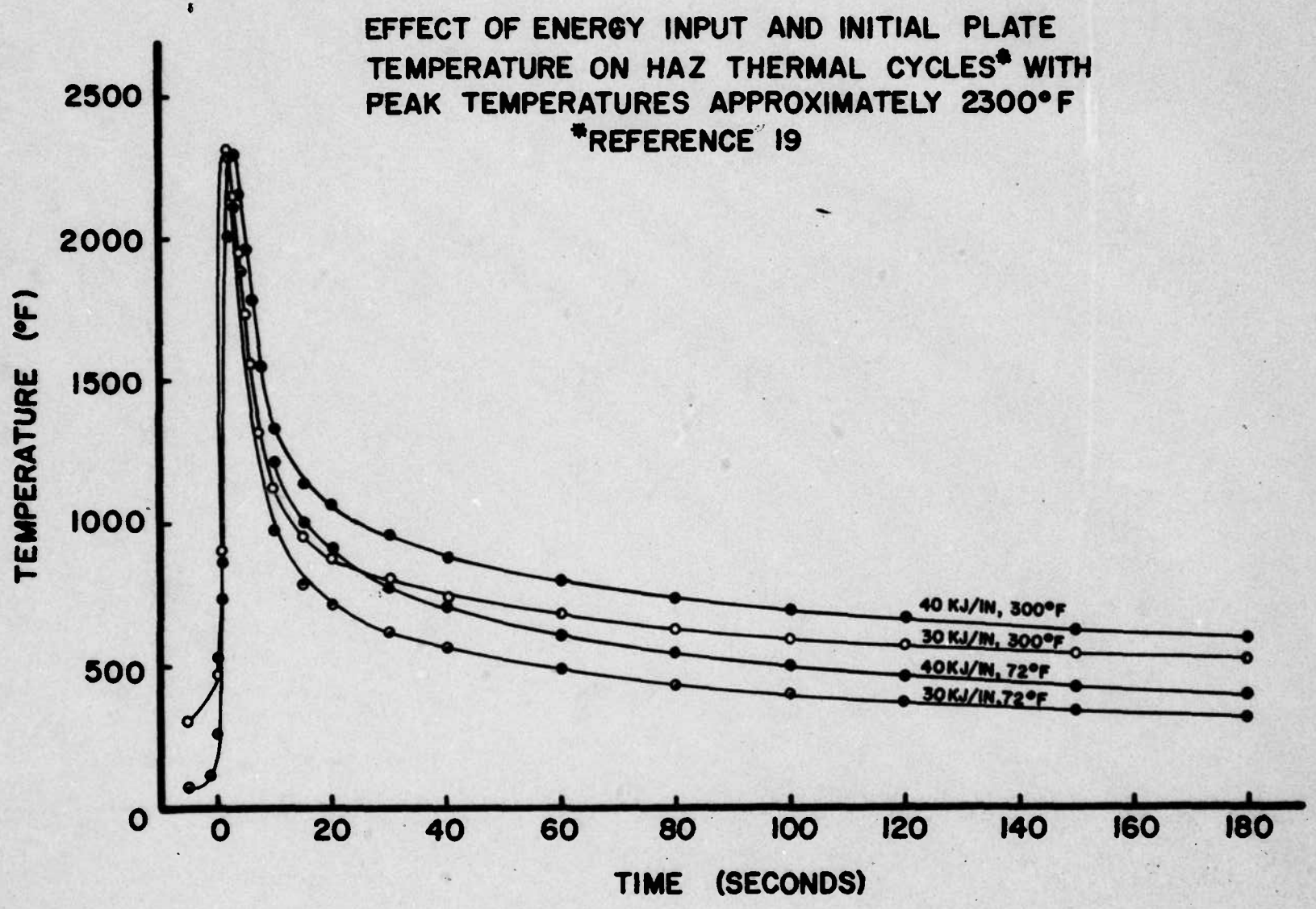
EFFECT OF ENERGY INPUT AND INITIAL PLATE TEMPERATURE ON HAZ THERMAL CYCLES* WITH PEAK TEMPERATURES APPROXIMATELY 2300°F
*REFERENCE 19
TEMPERATURE (°F)
2500
2000
1500
1000
500
0
0
20
40
60
80
100
120
140
160
180
TIME (SECONDS)
40 KJ/IN, 300°F
30 KJ/IN, 300°F
40KJ/IN, 72°F
30KJ/IN, 72°F

Figure 10

either to the postheating furnace or the liquid-nitrogen storage bath was approximately 3 minutes.

To check the effect of time and temperature on hydrogen content, the entire welding fixture was quenched immediately after a 40 kj/in. weld bead was deposited by the GMA process on a Heat-A test specimen preheated to 300°F. As expected, the initial hydrogen content of this specimen was much higher (12.2 ppm) than that obtained with the normal procedure (5.2 ppm), which involved the 3-min. transfer time. These results confirm that the cooling rate has a marked influence on the initial hydrogen level. In fact, the initial hydrogen level in the 40 kj/in. welds appears to have been reduced to the point where the experimental accuracy of the analytical technique makes it impossible to distinguish between the tail of an exponential curve and a linear plot.

The more rapid decrease in hydrogen content observed during postheat for welds made with 30 kj/in. can be explained by the fact that the weld bead produced was significantly smaller than that produced with 40 kj/in. Because the diffusion distance is significantly less, the time required to reduce the hydrogen content to an acceptably low level is greatly decreased.

Figure 9 summarizes the effect of energy input and postheat time on the hydrogen content of SMA welds. The term "contaminated" is used to describe SMA electrodes which were stored in ambient atmosphere to allow moisture pickup and then baked in a ventilated oven at 300°F to remove part of the moisture. The term "reconditioned" is used to describe SMA electrodes which were baked for 1 hr. at 775°F (413°C) to remove coating moisture as recommended by the manufacturer.

As mentioned above, the apparent "initial" hydrogen level for welds made using 40 kj/in. at 300°F is much lower than that for the welds made using 30 kj/in. at 300°F because of the difference in cooling rates. The fact that the lowest diffusible hydrogen levels were measured for a 40 kj/in. weld made with contaminated electrodes was disturbing until metallography revealed the presence of porosity in these welds. It has been demonstrated[20] that hydrogen diffuses into porosity where it reassociates into molecular form. As a consequence, at temperatures below about 200°C (392°F) the escape of the hydrogen requires weeks, rather than hours as would be the case in the absence of porosity. Thus, despite the fact that the total hydrogen content must be significantly higher in welds made with contaminated electrodes, the diffusible hydrogen evolved during the 72-hr. period in vacuum was reduced by the presence of porosity to the order of magnitude of the experimental error for the BWRA/IIW analytical procedure.

On the other hand, with 30 kj/in. energy input the faster cooling rates provide higher "initial" hydrogen levels and the weld deposits made with the reconditioned electrodes show lower diffusible hydrogen, as would be expected.

Table V summarizes the results of ASC tests made using 0.5% augmented strain on GMA welds of HY-130. Included in the table are:

1. the percent hydrogen added to the Ar-2% O_2
2. a coded symbol which indicates the presence or absence of hydrogen-induced cracking and identifies cracking by type as:
   a. weld metal only . . W
   b. initiating in weld metal and propagating into base metal . . . . . WB
   c. initiating in base metal and propagating into weld metal . . . . BW
   d. wholly contained within base metal (including unmixed zone) . . B
   e. macrocracks indicated by an *
   f. no cracking . . . N
3. the diffusible hydrogen level, which is included for convenience directly below the cracking symbols.

Table VI summarizes the same type of information for ASC tests made using 0.75% augmented strain on GMA welds.

Tables VII and VIII summarize the results of ASC tests on SMA welds using 0.5% and 0.75% augmented strain, respectively. The format is the same except the terms "contaminated" and "reconditioned" are substituted for the % hydrogen column.

The results listed in Tables V and VI for the GMA welds show that the level of hydrogen required to initiate cracking is inversely related to both the augmented strain and the hardness of the weld metal. At both 0.5% and 0.75% augmented strain levels, the 40 kj/in. welds showed no cracking when a 20-minute 300-^{o}F postheat treatment reduced the hydrogen content to less than 4 ppm. However, at 0.5% augmented strain both 30 kj/in. welds showed cracking until the postheat treatment reduced the hydrogen level below 2 ppm. At 0.75% augmented strain the 30 kj/in. welds continued to show cracking after a 30-minute 300-^{o}F postheat treatment which had reduced the hydrogen level to less than 1 ppm.

TABLE V

SUMMARY OF ASC TEST RESULTS ON GMA WELDS USING 0.5% AUGMENTED STRAIN

HEAT	ENERGY INPUT (kj/in)	% H_2 ADDED to Ar+2%O_2	NO PREHEAT	300°F PREHEAT POSTHEAT TIME at 300°F (min) 0	10	20	30
A	40	0.00	N 1.3	N 1.0	N 0.9	N 0.9	N 0.8
A	40	0.375	W,WB,B* 7.3	W,WB,B* 6.1	W 5.9	W,B 5.5	W 4.7
B	40	0.375	W 4.6	W 3.2	W 2.9	W 2.4	W 1.9
B	40	1.25	W --	W 5.0	N --	N --	N 3.3
A	40	2.5	W,B,WB* 6.2	W,B,BW,WB* 5.2	W 4.8	W --	W 4.1
B	40	2.5	W,WB* 5.5	W,WB* 4.4	N --	N 3.7	N 3.4
A	30	2.5	W,WB* 9.3	W,B,WB* 7.8	W 2.2	N 1.2	N 0.8
B	30	2.5	W,WB* --	W,WB* 6.1	W 2.2	N 1.3	N 0.7

See text for definition of symbols * Macrocracks

TABLE VI

SUMMARY OF ASC TEST RESULTS ON GMA WELDS USING 0.75% AUGMENTED STRAIN

HEAT	ENERGY INPUT (kj/in)	% H_2 ADDED to Ar+2%O_2	NO PREHEAT	300°F PREHEAT POSTHEAT TIME at 300°F (min) 0	10	20	30
A	40	0.00	N 1.3	N 1.0	N 0.9	N 0.9	N 0.8
A	40	0.375	W,BW* 7.3	W,WB* 6.1	W 5.9	W,B 5.5	W,B 4.7
B	40	0.375	W,B,WB* 4.6	W,WB* 3.2	N 2.9	N 2.4	N 1.9
B	40	1.25	W --	W,WB* 5.0	N --	N --	N 3.3
A	40	2.5	W,B,WB* 6.2	W,B,WB* 5.2	B 4.8	N --	W 4.1
B	40	2.5	W,WB* 5.5	W,WB* 4.4	N --	N 3.7	N 3.4
A	30	2.5	W,WB* 9.3	W,WB* 7.8	W 2.2	W 1.2	W 0.8
B	30	2.5	W,WB* --	W,WB* 6.1	W 2.2	W 1.3	W 0.7

* Macrocracks

TABLE VII

SUMMARY OF ASC TEST RESULTS ON SMA WELDS USING 0.5% AUGMENTED STRAIN

HEAT	ENERGY INPUT (kj/in)	ELECTRODE MOISTURE CONDITION	NO PREHEAT	300°F PREHEAT POSTHEAT TIME at 300°F (min) 0	10	20	30
A	30	Contaminated	W,WB*	W,WB*	W	N	N
			8.0	7.7	--	2.5	1.0
B	30	Contaminated	W*	W*	W	N	N
			--	7.4	6.6	2.5	1.0
A	40	Contaminated	W,WB*	W,WB*	W	W	W
			--	2.0	1.8	1.5	1.3
B	40	Contaminated	W*	W,WB*	N	N	N
			2.4	--	0.7	0.5	0.5
A	30	Reconditioned	N	N	N	N	N
			7.1	5.8	2.7	2.1	1.7
B	30	Reconditioned	W	W	N	N	N
			6.0	4.2	1.5	0.8	0.5
A	40	Reconditioned	N	N	N	N	N
			3.7	2.2	1.9	1.9	1.5

See text for definition of symbols * Macrocracks

TABLE VIII

SUMMARY OF ASC TEST RESULTS ON SMA WELDS USING 0.75% AUGMENTED STRAIN

HEAT	ENERGY INPUT (kj/in)	ELECTRODE MOISTURE CONDITION	NO PREHEAT	300°F PREHEAT POSTHEAT TIME at 300°F (min) 0	10	20	30
A	30	Contaminated	W,WB 8.0	W,BW* 7.7	W --	N 2.5	N 1.0
B	30	Contaminated	W* --	W,WB* 7.4	W 6.6	N 2.5	N 1.0
A	40	Contaminated	W,WB* --	W,WB* 2.0	W 1.8	W 1.5	N 1.3
B	40	Contaminated	W* 2.4	W,WB* --	W* 0.7	N 0.5	N 0.5
A	30	Reconditioned	W 7.1	W 5.8	W 2.7	N 2.1	N 1.7
B	30	Reconditioned	W 6.0	N 4.2	N 1.5	N 0.8	N 0.5
A	40	Reconditioned	N 3.7	N 2.2	N 1.9	N 1.9	N 1.5

* Macrocracks

The results listed in Tables VII and VIII for the SMA welds show a similar dependence of the level of hydrogen required to initiate cracking upon both the augmented strain and weld hardness. The welds made using 40 kj/in. with reconditioned electrodes in Heat A showed no cracking with 0.75% augmented strain even when no preheat was employed, which resulted in a hydrogen level of 3.7 ppm. However, at the same augmented strain the 30 kj/in. welds made with reconditioned electrodes in Heat A showed cracking even when postheat treatment had reduced the hydrogen level to 2.7 ppm.

The lower tolerance for hydrogen of the 30 kj/in. welds can be attributed to the harder, more crack-susceptible microstructure produced by the faster cooling rate. Figure 11 shows the measured hardness across weld beads produced with the two energy inputs. Note that the hardness of the weld made with 30 kj/in. is consistently higher than that at similar locations in welds made with 40 kj/in.

Except for the specimens obtained from one GMA weld in Heat B (third horizontal row in Tables V & VI), no cracking was observed in GMA welds which contained less than 4 ppm of hydrogen. This weld was made under the same conditions as the companion weld in Heat A (second horizontal row in Tables V & VI), but exhibited a different weld contour. The droplet size was smaller in the weld on Heat B, and the bead was broader and flatter. The weld in Heat A exhibited a higher crown and some unfused overlap at the sides. It is postulated that the difference in bead contours and droplet size may have influenced the test results.

An instability in the arc-transfer mode could influence the contour and hydrogen pickup from point to point along the weld. However, only a single hydrogen analysis was used to categorize both strain levels. In other words, the ASC specimens do not necessarily have the same hydrogen content as the specimen used for analysis. This emphasizes the need for a rapid method of measuring diffusible hydrogen. If such a method were available, a statistically significant average hydrogen content could be obtained, and the effects of such variables as droplet size and bead contour could be studied.

The results listed in Tables V, VI, VII, and VIII show that cracking was found predominately within the weld metal, as is to be expected in HY-130 weldments. In specimens welded without postheat treatment, several of these weld-metal cracks were found to propagate into the base metal. Crack initiation within the base metal was found to be much more prevalent in Heat A

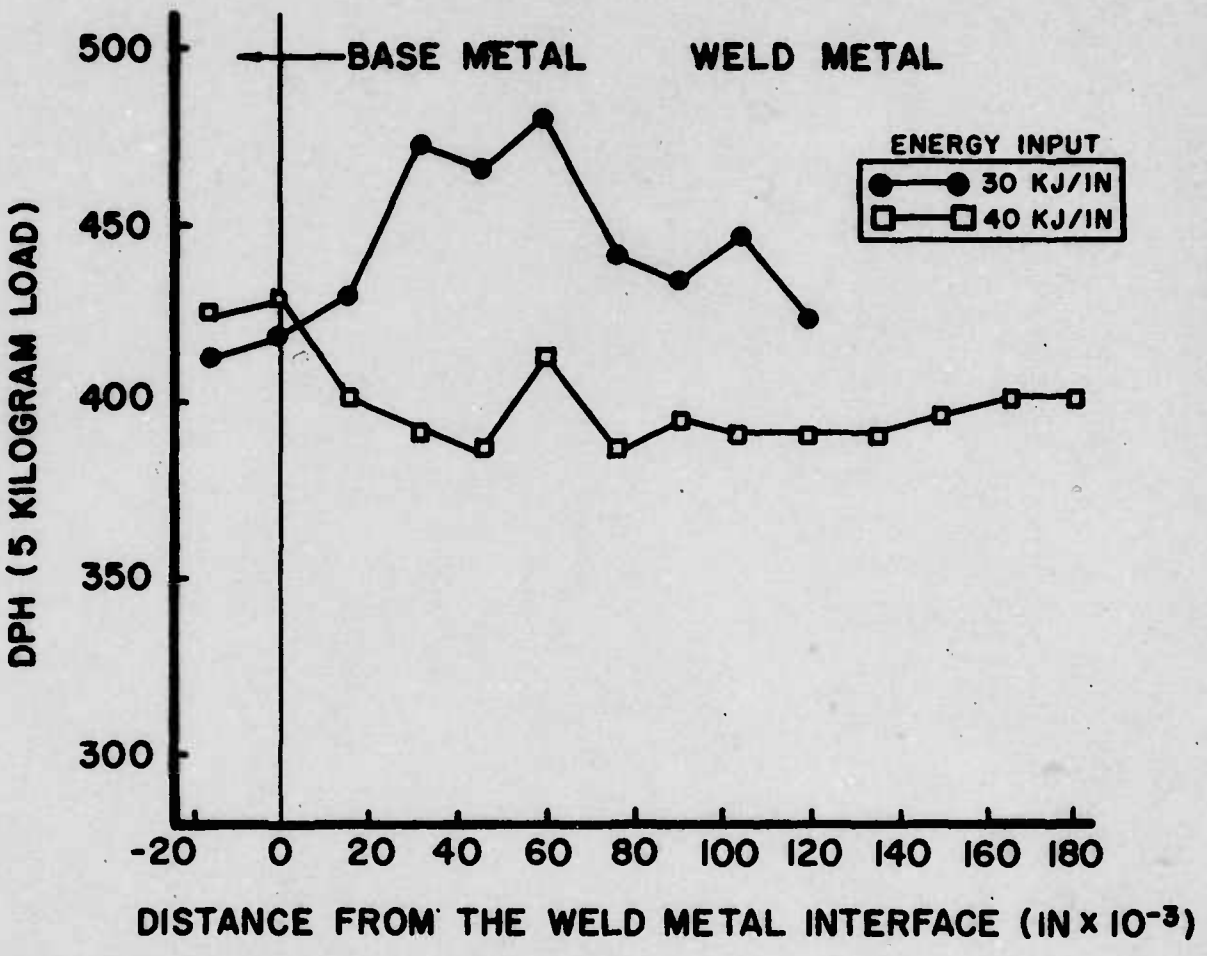

Figure 11

Measured Hardness across Weld Beads from the Two Energy Inputs Used, 300°F Preheat.

than Heat B. In fact, only one incidence of crack initiation within the heat-affected zone (HAZ) of Heat B was found. In this one incidence, a small crack initiated at a nonmetallic inclusion in a specimen welded without either preheat or postheat treatment and tested with an applied augmented strain of 0.75%. The differences in the base-metal cracking tendencies of the two heats of HY-130 will be discussed in more detail in the following section.

The Role of Microstructure

a. Crack initiation and propagation studies. As indicated earlier in Tables V, VI, VII, and VIII, cracking was observed in both the weld metal and the HAZ of the base metal. While cracking in the weld metal was predominately intergranular, cracking in the HAZ was found to be a mix of intergranular and transgranular.

The photomicrograph in Fig. 12, taken at 500X, shows the typical appearance of cracking associated with the prior austenitic grain boundaries in the weld metal. Generally, cracks were found to initiate in the weld metal and to propagate into the HAZ. However, on occasion, cracking initiated at sulfide inclusions within the partially melted zone or the adjacent HAZ and propagated into the weld metal. The effects of sulfide inclusions and banding upon HAZ cracking will be discussed later in this section. Figure 13, taken at 75X, shows a macrocrack which initiated in the weld metal and propagated into the HAZ.

Szekeres[21] showed that the fusion boundary of a weld is comprised of four distinct regions: the composite zone, the unmixed zone, the partially melted zone, and the true heat-affected zone (HAZ). Szekeres also proposed a mechanism for crack nucleation in the unmixed zone. He hypothesized that the increased solubility in austenite during transformation of the composite zone could increase the hydrogen concentration of the unmixed zone. The composite zone, being lower in carbon and alloy content, would transform to martensite at a higher temperature than the unmixed zone. As the composite zone transformed to martensite, it therefore would reject hydrogen to the as-yet untransformed unmixed zone. This partitioning process could increase the concentration of hydrogen in the unmixed zone. Thus, the unmixed zone would be a likely site for crack nucleation.

Figure 14 seems to confirm Szekeres' hypothesis. Note the small microcrack along the solidification grain boundary in the unmixed zone at A.

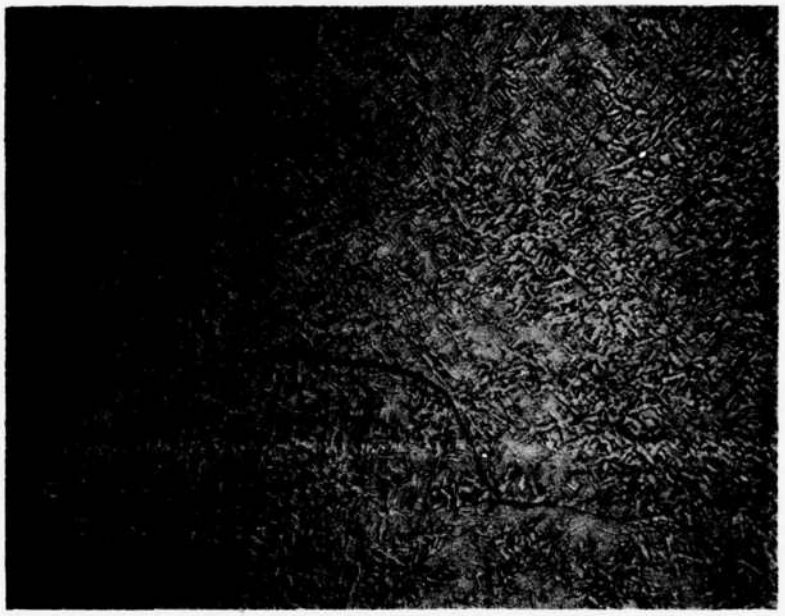

Figure 12

Typical Appearance of Cracking Associated with Prior Austenite Grain Boundaries in the Weld Metal. Etching Procedure A, 500X.

Figure 13

Macrocrack which Initiated in the Weld Metal and Propagated into the Heat-Affected Zone. Etching Procedure B, 75X.

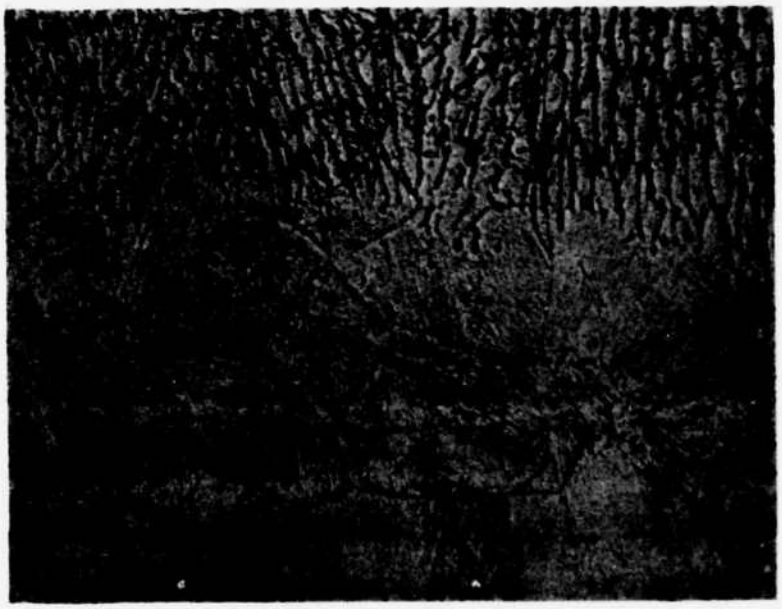

Figure 14

Microcrack Initiation along the Solidification Grain Boundary in the Unmixed Zone at A.
Etching Procedure B, 500X.

b. Nucleation of hydrogen-induced cracks by non-metallic inclusions. Hydrogen-induced cracking was found to be associated with non-metallic inclusions in the HAZ and partially melted zone of both heats of HY-130. As previously stated, Heat A exhibited a greater number of elongated inclusions near the plate midthickness than did Heat B. This fact may account for the fewer HAZ cracks nucleated in Heat B.

This result also supports Szekeres'[21] findings for HY-80. He suggested that the shape and size of sulfide inclusions could influence the nucleation of cold cracks in different heats of the same grade of steel, even though the volume fraction of the sulfides in the heats were equal. He argued that the amount of hydrogen necessary to cause a sulfide inclusion to become a crack initiator was a function of how effective the inclusion was as a stress raiser. Large, thin, ellipsoidal sulfide inclusions with their long axes perpendicular to the principal stress would be extremely effective in nucleating cracks in the HAZ of welds in martensitic steels. Furthermore, such large, flat inclusions would be more effective than globular inclusions in pinning moving grain boundaries in the HAZ during welding. If prior austenite grain boundaries became aligned with elongated sulfides, an especially effective crack-initiation site would result because hydrogen could arrive at the triaxially stressed region more readily via the grain boundaries.

Observation of the specimen surface during the ASC test confirmed the fact that elongated sulfide inclusions in Heat A were effective stress concentrators. Microscopic examination during the tests revealed a region of localized yielding near the tips of the elongated non-metallic inclusions. No such localized yielding or surface roughing was observed to be associated with spherical inclusions in either heat. Homma[22] observed and photographed similar localized yielding associated with inclusions during ASC testing of HY-80.

Figure 15 shows a typical example of a macrocrack nucleation by a typical elongated sulfide inclusion in the HAZ of a weld bead in a specimen from Heat A. Although this crack did not propagate farther, similar cracks from elongated sulfide inclusions were observed to propagate into and even through the weld metal.

Accoustic-emission results confirm the effect of an elongated sulfide inclusion on the time for crack initiation and fracture in an ASC specimen tested with 0.5% strain. Figure 16 is a plot of acoustic-emission counts vs time taken during ASC testing of 2 specimens of Heat A subjected

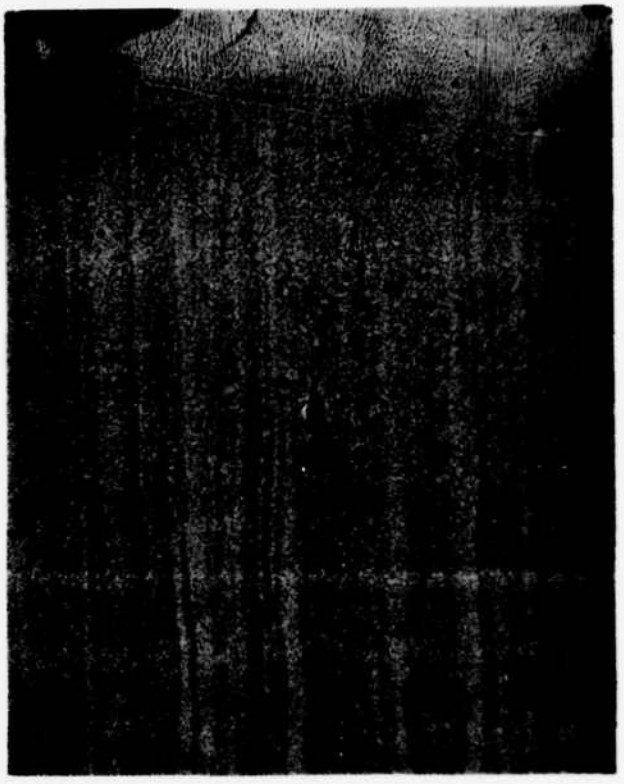

Figure 15

Typical Macrocrack Nucleation by a Elongated Sulfide Inclusion in the Heat-Affected Zone of a Weld Bead in Heat A. Etching Procedure A, 50X.

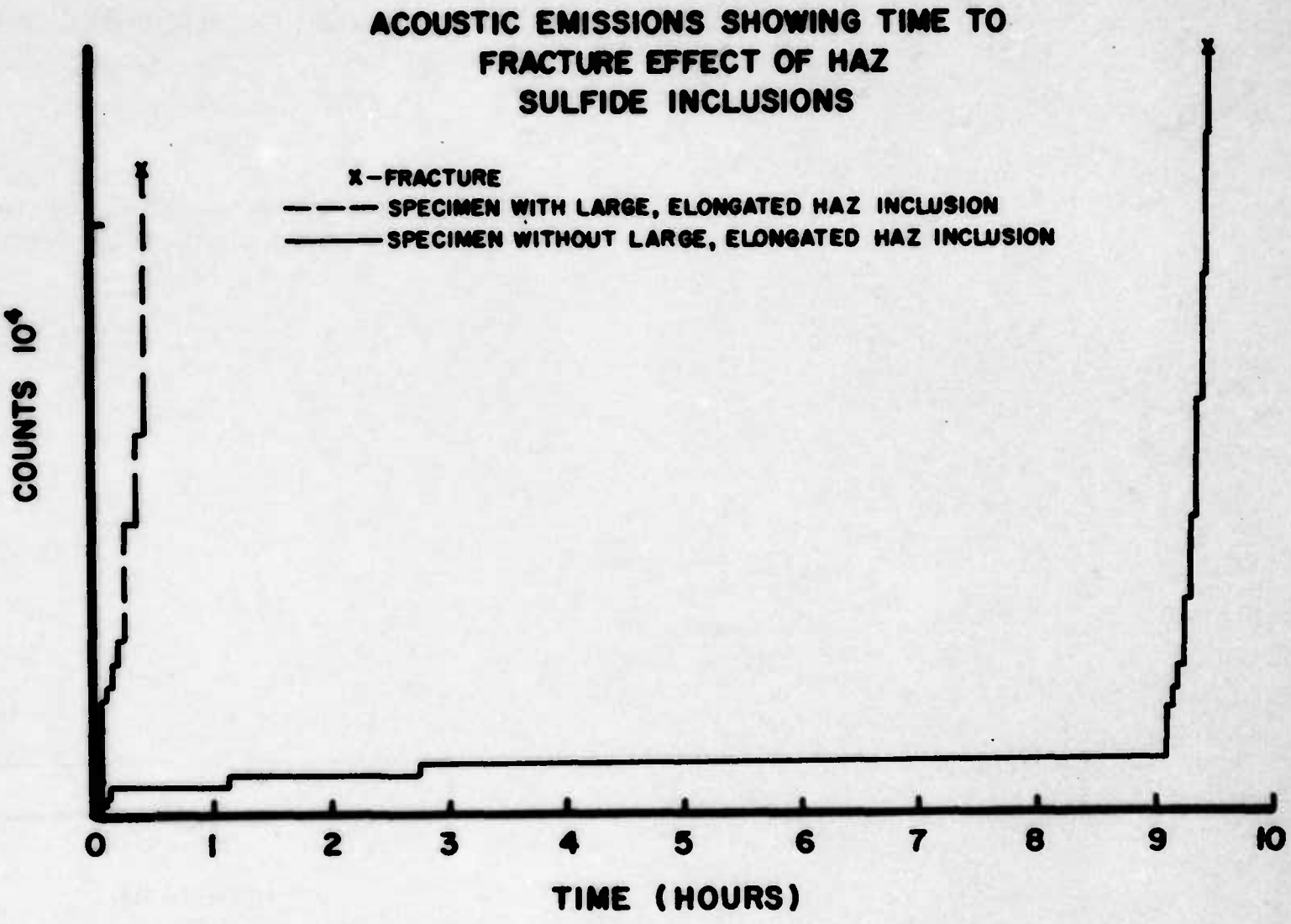
ACOUSTIC EMISSIONS SHOWING TIME TO
FRACTURE EFFECT OF HAZ
SULFIDE INCLUSIONS
X-FRACTURE
SPECIMEN WITH LARGE, ELONGATED HAZ INCLUSION
SPECIMEN WITHOUT LARGE, ELONGATED HAZ INCLUSION
COUNTS 10⁴
0
1
2
3
4
5
6
7
8
9
10
TIME (HOURS)

Figure 16

to the same weld-pass, preheat, and postheat treatments. Crack initiation in the specimen with a large elongated inclusion in the HAZ occurred almost immediately after application of load, and propagation to failure required less than 30 mins. Subsequent metallographic examination revealed that no such large inclusions were present in the other specimen of Heat A. In this specimen, nucleation was retarded significantly and propagation to failure required nearly 10 hrs. Figure 17, a, b, and c, show several examples of microcracking extending from non-metallic inclusions in both heats of HY-130. Note that while cracking associated with these inclusions was predominately intergranular, in a few instances the cracks were able to propagate across grains. Also, note the plastic flow of the metal matrix surrounding the elliptical inclusions shown in Fig. 17c.

It has been reported[23] that manganese-sulfide inclusions in the base metal can react with explosive violence during welding and create gas pockets at the fusion boundary. Szekeres[21] postulated that such microvoids would be excellent traps for any hydrogen present and, therefore, could become excellent crack-initiation sites. Figure 18 shows a macrocrack propagated from such a microvoid formed in the partially melted zone.

c. Influence of banding upon heat-affected zone cracking. Metallographic examination revealed that the two heats of HY-130 were heavily banded. Figure 19 shows typical banding as revealed by a solute-sensitive etchant. The light-etching bands are higher in alloy content than the dark-etching bands, and thus correspond to the regions last to freeze between the dendritic arms in the original ingot. During subsequent hot-rolling, these segregated regions are converted to bands which are not eliminated by normalizing treatments.

Szekeres[21] in his study of hydrogen cracking in HY-80 showed that the orientation of these bands with respect to the principal stress direction had a considerable effect upon the degree of cold cracking in the HAZ. In specimens with banding parallel to the stress direction, cracking in the true HAZ was virtually eliminated, while specimens with banding transverse to the stress direction showed hydrogen-induced cracking in the alloy-rich bands.

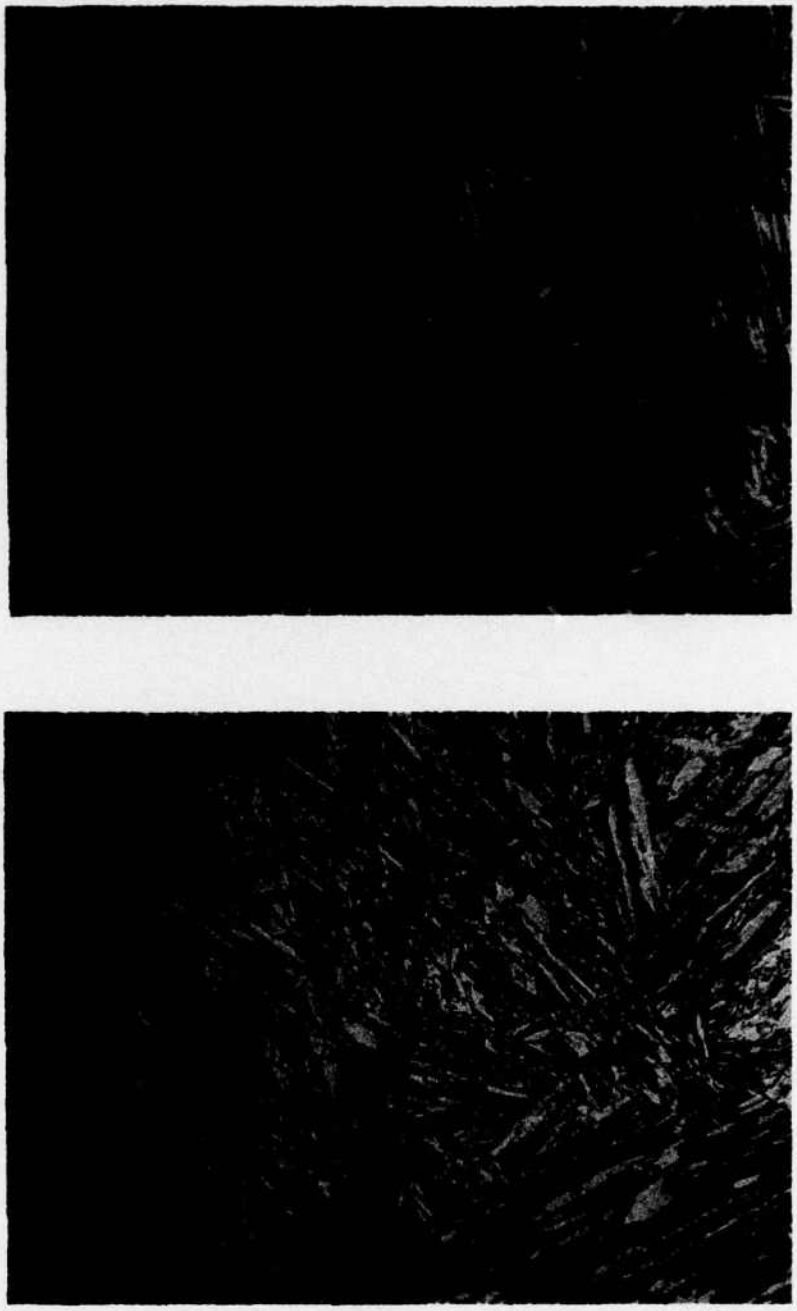

Figure 17a

Microcracking Associated with Sulfide Inclusions in Heat B. Etching Procedure B.
Top: 250X
Bottom: 500X

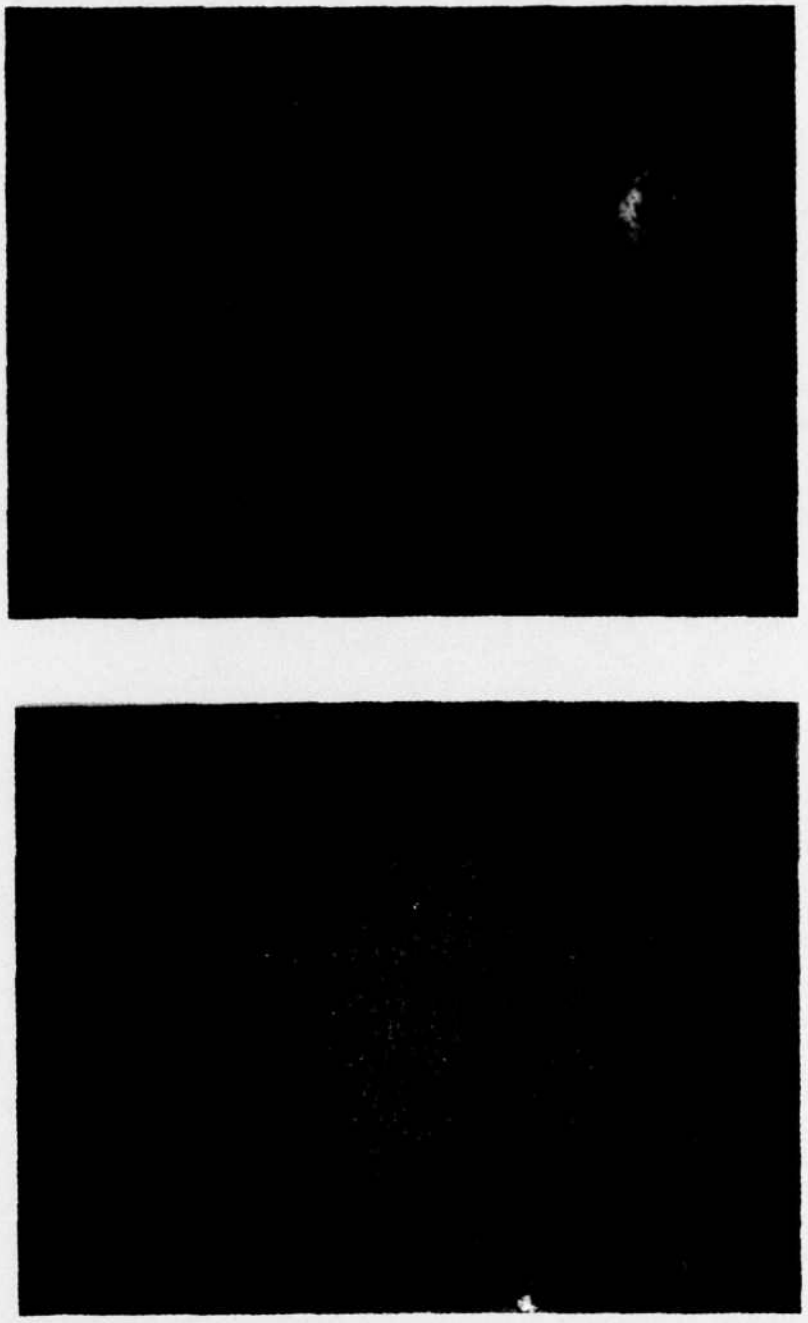

Figure 17b

Microcracking from Inclusions following Prior Austenite Grain Boundaries. Etch Procedure B, 500X.

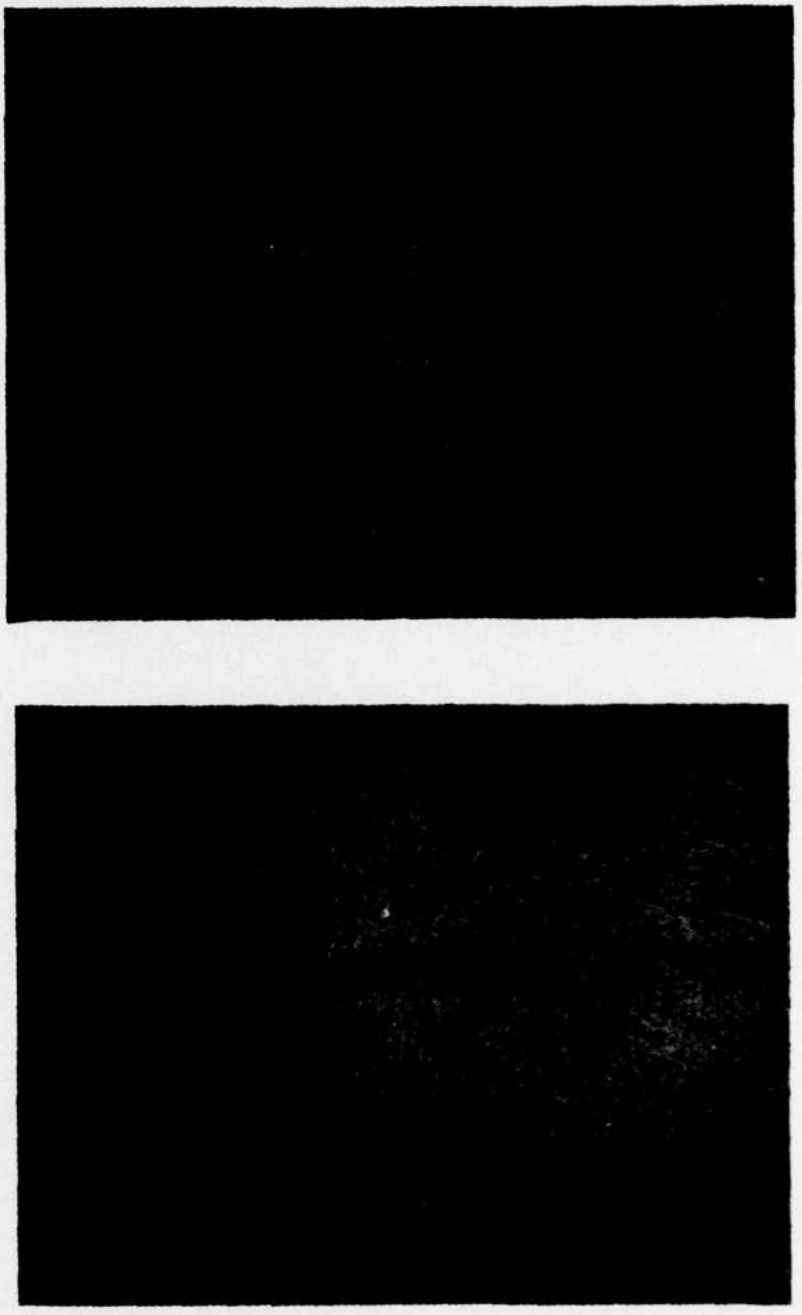

Figure 17c

Microcracking from Inclusions Showing Transgranular and Intergranular Cracking. Etch Procedure B, 500X.

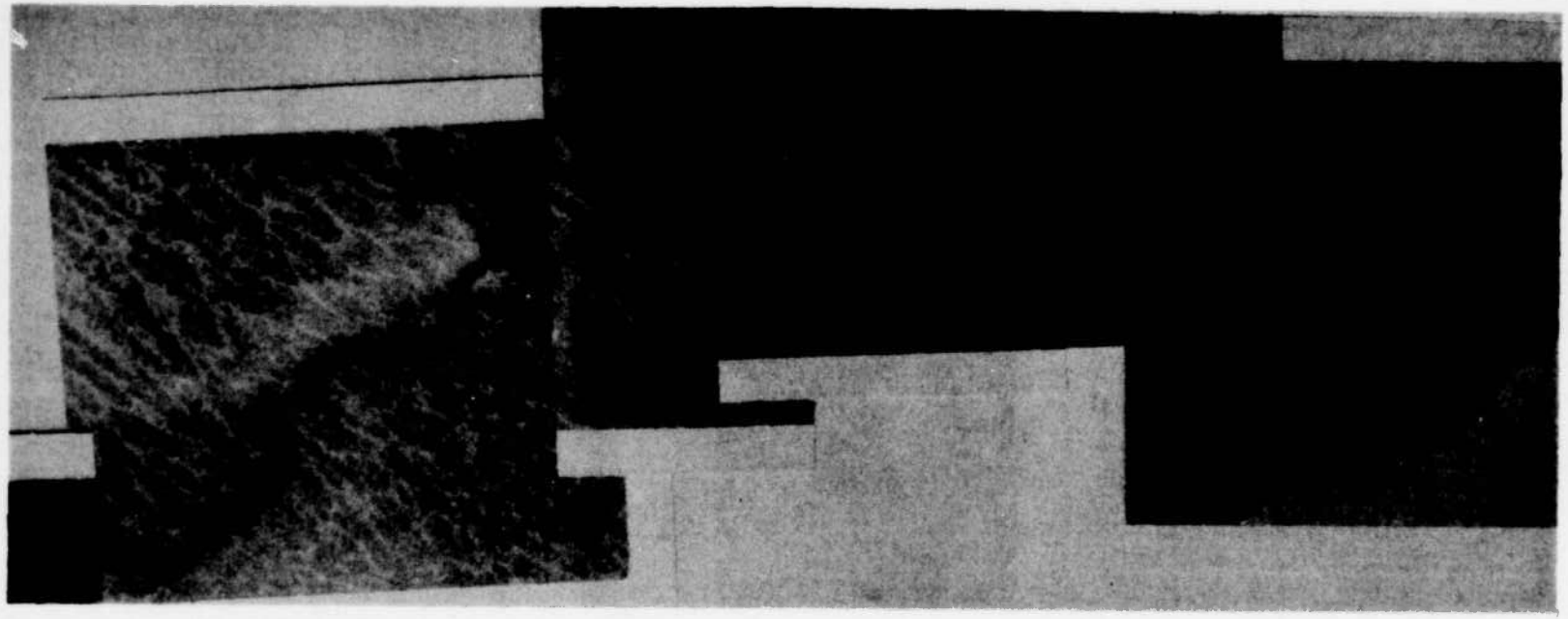

Figure 18

Macrocrack Initiation and Propagation from a Microvoid along a Sulfide Inclusion in the Partially Melted Zone. Etch Procedure A, 150X.

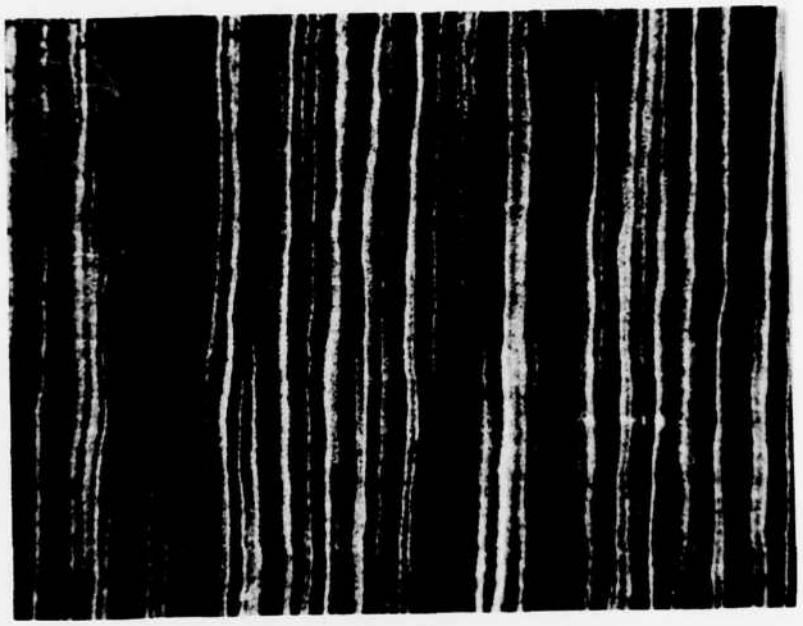

Figure 19

Typical Banding in Both Heats of HY-130. Etch Procedure A, 100X.

Szekeres[21] attributed the low incidence of cracking in specimens with the parallel banding-to-stress orientation to the observation that the elongated sulfides always found in the alloy-rich bands (Fig. 20) were the primary nuclei for cracks. With the parallel orientation, the long axes of the sulfides were parallel to the stress direction, and therefore, were less effective as stress raisers. Thus, crack nucleation was either reduced or eliminated.

The same relationship between banding and the orientation of the elongated sulfides was observed in HY-130 investigation. Therefore, all specimens used in this investigation were tested with banding transverse to the principal stress direction. The results confirmed Szekeres' findings[21] that most true HAZ cracks in specimens were observed to be within the light-etching bands. However, grain-boundary microcracks were found in light-etching bands within the true HAZ where no elongated sulfide inclusions were present on the surface observed. Figure 21 shows typical examples of such cracks.

Tokunaga[24] showed that in many instances cracking in ASC specimens initiated at elongated inclusions just beneath the surface and propagated rapidly to the exposed surface. Thus, the fact that no sulfide is visible on the surface does not rule out the possibilities that an elongated sulfide served as the initiation site.

In addition, Fig. 22, taken from the work of Sawhill[1], shows that the hardness of these alloy-rich bands is significantly higher than that of the solute-lean bands.

Acoustic-Emission Studies

The acoustic-emission monitoring apparatus permitted study of the crack-initiation and propagation behavior during the ASC tests. The total number of stress-wave emissions were recorded as a function of time with an X-Y recorder.

In the welds with high hydrogen contents, crack initiation, propagation, and fracture generally occurred within a few minutes after loading. The total number of stress-wave emissions from both the 0.5% and 0.75% strained specimens appeared to be approximately equal. According to Hartbower[17], this behavior indicates that the extent of crack propagation within specimens was essentially the same for both levels of augmented strain. Homma,[22]

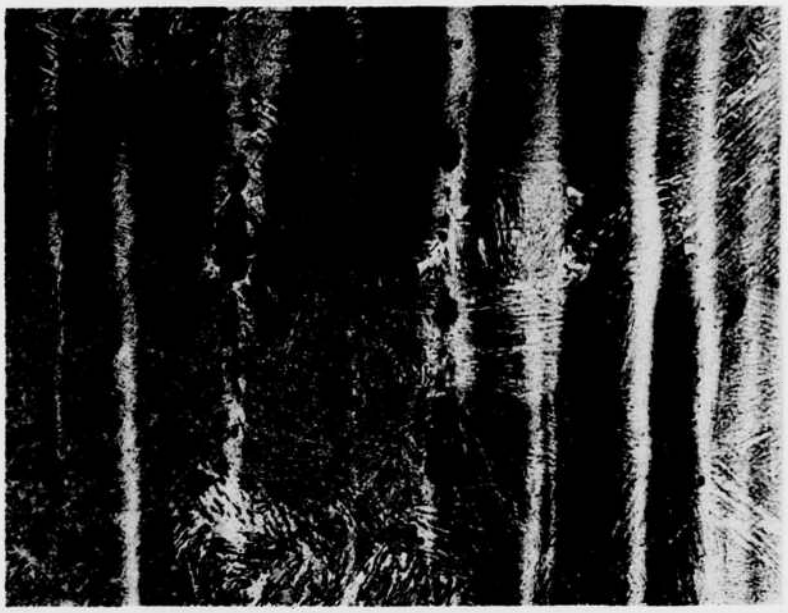

Figure 20

Elongated Non-metallic Inclusions Found in Alloy-Rich Bands of the Base Metal. Etch Procedure A, 500X.

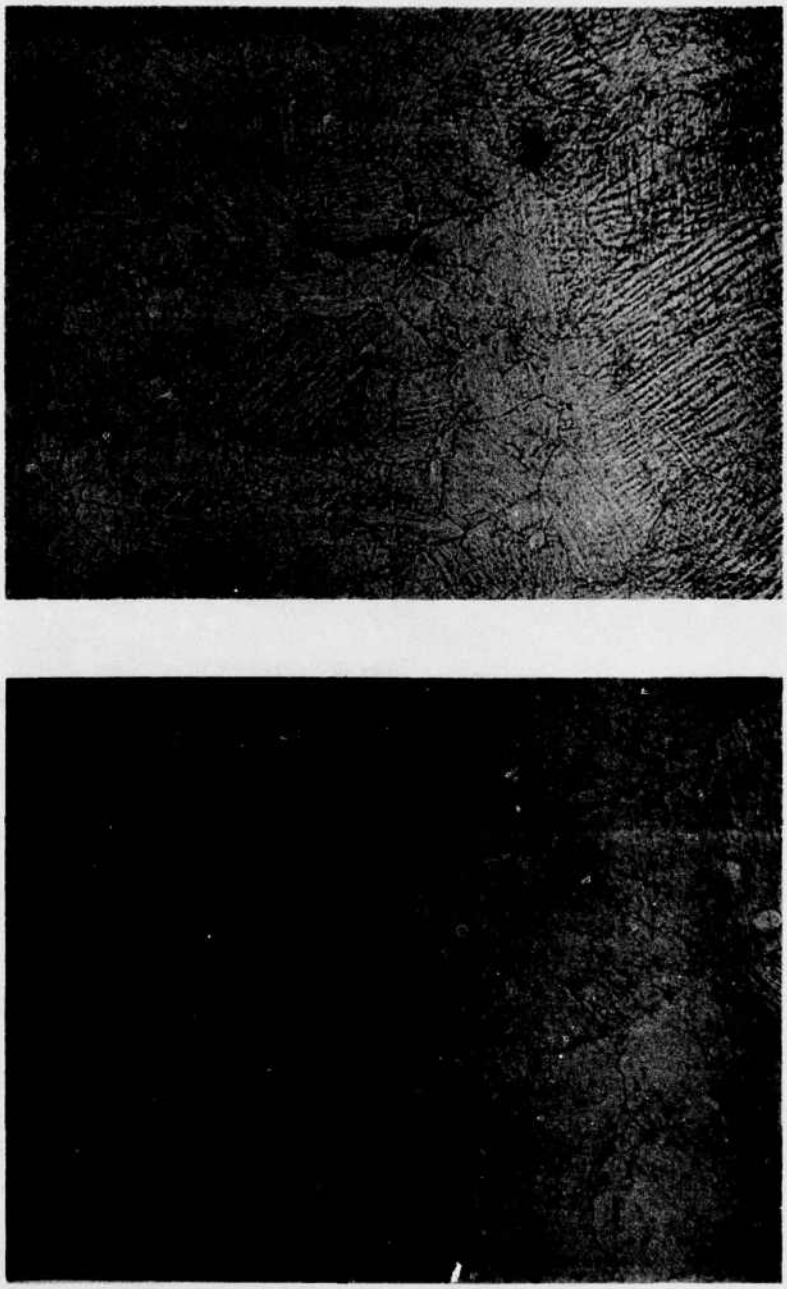

Figure 21

Grain-Boundary Microcracks Found in Alloy-Rich Areas of the True Heat-Affected Zone. Etch Procedure B.
Top: 250X
Bottom: 500X

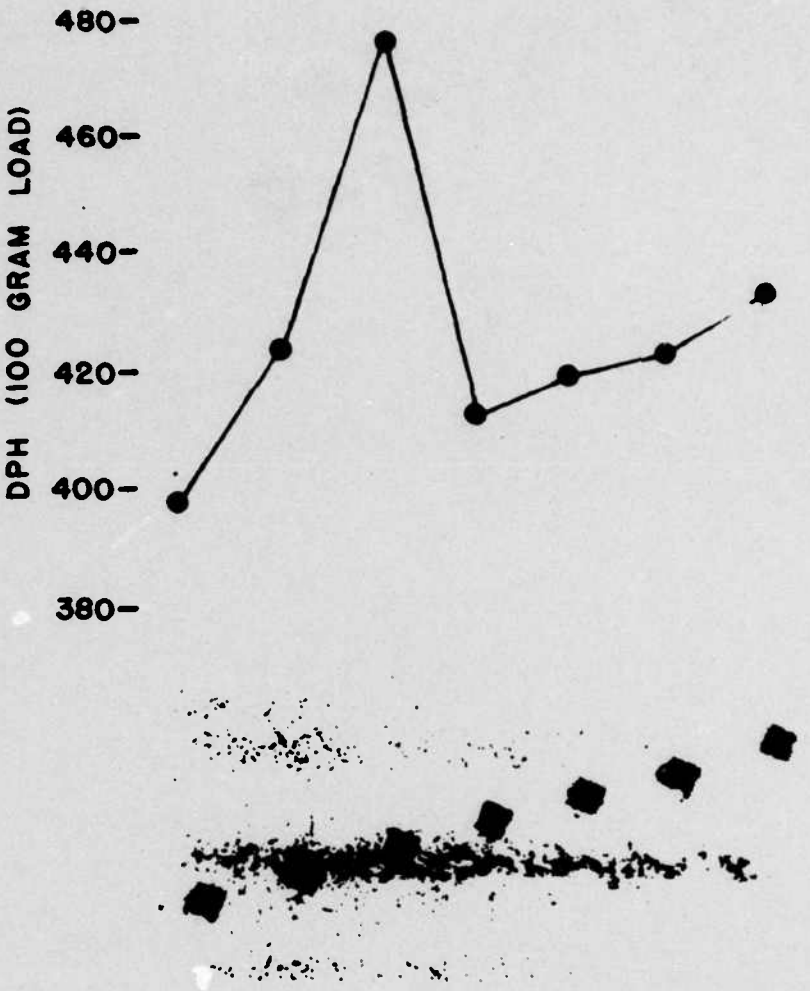

Figure 22

Hardness Transverse Across Bands in an HY-130 Heat-Affected Zone, DPH, 100 gm. load. Picric Acid Etch, 200X. The picric acid etch darkens solute rich areas whereas etch procedure A darkens solute lean areas.

in testing ASC specimens of HY-80, found that both the area experiencing plastic deformation and the width of the main crack increased as the amount of augmented strain increased. However, he found that the total length of the cracks was relatively insensitive to the augmented strain imposed on the specimens. Therefore, the acoustic-emission results found in this investigation would appear to confirm Homma's findings in HY-80.

In general, as the hydrogen content of the welds was decreased, the time required for crack initiation increased and the rate of crack propagation decreased. Ultimately, below a critical hydrogen level, the specimens did not fracture and at very low levels, no cracking occurred. As noted previously, the level of hydrogen required to initiate cracking was found to be inversely related to both augmented strain and the weld hardness.

In summary, the acoustic-emission tests proved to be a valuable aid for evaluating the cracking observed in the ASC test.

CONCLUSIONS

The conclusions drawn from this investigation of weldments in two HY-130 steels, utilizing the augmented strain cracking (ASC) test, are:

1. No hydrogen-induced cracks were observed when the augmented strain was such as to produce stresses significantly below the yield strength regardless of energy input, preheat, or postheat practice.
2. The use of a combination of 300^{0}F preheat and postheat was effective in lowering the diffusible hydrogen content of weldments.
3. With one exception, no hydrogen-induced cracking was observed in GMA welds made at 40 kj/in. and containing less than 4 ppm diffusible hydrogen.
4. Except for welds containing hydrogen porosity, no cracking was observed in SMA welds made at either 40 kj/in. or 30 kj/in. and containing less than 2.5 ppm of diffusible hydrogen.

5. The presence of hydrogen porosity appears to decrease the amount of diffusible hydrogen as measured by the BWRA/IIW analysis. The porosity presumably acts as "traps" (recombination sites) for the hydrogen.

6. The measured level of diffusible hydrogen required to cause cracking in specimens containing porosity is significantly lower than that required in the absence of porosity.

7. Hydrogen-induced cracking in HY-130 weldments initiated predominately in the weld metal, although some microcracks were found within the heat-affected zone of the base metal when sufficient hydrogen was present.

8. Some hydrogen-induced cracks initiated at grain boundaries in the unmixed and/or partially melted zone and propagated into the weld metal. However, most cracks which propagated across the weld fusion line initiated in the weld metal.

9. Many hydrogen-induced cracks initiated at elongated non-metallic inclusions, which were predominantly manganese sulfides.

10. Elongated inclusions with their long axes perpendicular to the stress, serve as preferential initiation sites for hydrogen-induced cracking.

11. Stubby or spherical inclusions are less effective nucleation sites.

12. Both heats of HY-130 steel showed pronounced bands of solute segregation parallel to the rolled surface.

13. Non-metallic inclusions were located preferentially in, and parallel to, the alloy-rich bands.

14. Hydrogen-induced cracking initiates and propagates more readily within the solute-rich bands.

15. The hydrogen content required to initiate cracking is inversely related to both the augmented strain and the hardness of the weld metal. Increasing the weld hardness by decreasing the GMA weld energy-input from 40 kj/in. to 30 kg/in. reduced the maximum allowable hydrogen to avoid cracking to less than 1.5 ppm with 0.5% augmented strain. With 0.75% augmented strain, cracking was observed with as little as 0.7 ppm of hydrogen.

16. Except for the GMA welds made with 30 kj/in., increasing the augmented strain from 0.5 to 0.75% did not alter the level for hydrogen required to induce cracking.

17. Anelastic deformation and surface roughening were observed at the tips of propagating cracks.

LITERATURE CITED

1. Sawhill, J. M., Dix, A. W., Savage, W. F., "Modified Implant Test for Studying Delayed Cracking," Welding Journal, 53 (12), Res. Suppl. 554-559 (1974).

2. Gross, J. H., "The Development of Steel Weldments," Welding Journal, 47 (6), Res. Suppl., 241-270 (1968).

3. Howden, D. G., Smith, E. G., Evans, R. M., "Hydrogen in HY-130 Weld Metal," Annual Report NR 031-770 (2), Battelle Columbus Laboratories, Columbus, Ohio (1976).

4. Delong, W. T., "Eliminating Hydrogen Cracking", Metal Progress, 94 (5), 74-78 (1968).

5. Graville, B. A., "Effect of Hydrogen Concentration on Hydrogen Embrittlement," British Welding Journal, 15 (6), 10-14 (1968).

6. Interrante, C. G. and Stout, R. D., "Delayed Cracking in Steel Weldments," Welding Journal, 43 (4), Res. Suppl., 145-160 (1968).

7. Robbins, L., "Report of Semi-Automatic Inert Gas Metal Arc Welding HY-80 Steel Out-of-Position," Conference Proceedings, U. S. Navy Bureau of Ships, Washington, D. C., 110-132 (1960).

8. Zapffe, C. A. and Sims, C. E., "Hydrogen Embrittlement, Internal Stresses and Defects in Steel," Trans. AIME, 145, 225-261 (1941).

9. Tetelman, A. S., "Fracture of Solids," Wiley and Sons, New York (1962).

10. Petch, N. J., "The Lowering of Fracture-Stress Due to Surface Adsorption," Phil. Mag., 1, 331-337 (1956).

11. Williams, D. P., and Nelson, H. G., "Embrittlement of 4130 Steel by Low Pressure Gaseous Hydrogen," Metallurgical Trans., 1 (1), 63-68 (1970).

12. Barth, C. F. and Steigerwald, E. A., "Evaluation of Hydrogen Embrittlement Mechanisms," Metallurgical Trans., 1 (12), 3451-3455 (1970).

13. Troiano, A. R., The Role of Hydrogen and Other Interstitials in the Mechanical Behavior of Metals," Trans. ASM, 52 (1), 54-80 (1960).

14. Beachem, C. D., "A New Model for Hydrogen Assisted Cracking (Hydrogen Embrittlement)," Metallurgical Trans., 3 (2), 437-451 (1972).

15. Steinman, J. B., Van Ness, H. C., and Ansell, G. S., "The Effect of High Pressure Hydrogen Upon the Notch Tensile Strength and Fracture Mode of 4140 Steel," Welding Journal, 44 (5), Res. Suppl., 221-224 (1965).

16. Bernstein, I. M., "The Role of Hydrogen in the Embrittlement of Iron and Steel", Materials Science Eng., 6 (1), 1-19 (1965).

17. Hartbower, C. E., Gerberich, W. W., Crimmons, P. P., "Monitoring Subcritical Crack Growth by Detection of Elastic Waves," Welding Journal, 47 (1), Res. Suppl., 1-18 (1968).

18. Coe, F. R., "Hydrogen in Weld Metal," BWRA Bulletin, 8, 76-81 (1967).

19. Nippes, E. F., Merrill, L. L., and Savage, W. F., "Cooling Rates in Arc Welds in ½-In. Plate," Welding Journal, 28 (11), Res. Suppl., 556-564 (1949).

20. Moreton, J., Coe, F. R., and Boniszewski, T., "Hydrogen Movement in Weld Metals," Metal Construction, 3, (5), 185-187 (1971).

21. Savage, W. F., Nippes, E. F., and Szekeres, E. S., "Hydrogen-Induced Cracking in Low-Alloy Steel," Welding Journal, 55 (9), Res. Suppl., 276-283 (1976).

22. Savage, W. F., Nippes, E. F., and Homma, H., "Hydrogen-Induced Cracking in HY-80 Weldments," Welding Journal, 55 (11), Res. Suppl., 368-376 (1976).

23. Lyman, T., Editor, Metals Handbook, 1948 Edition, The American Society for Metals, Cleveland, Ohio (1948).

24. Tokunaga, Y., "Hydrogen-Assisted Cracking in HY-130 Steel," Master's Thesis, Rensselaer Polytechnic Institute, Troy, N. Y., January 1974, to be published, Welding Journal, Res. Suppl.

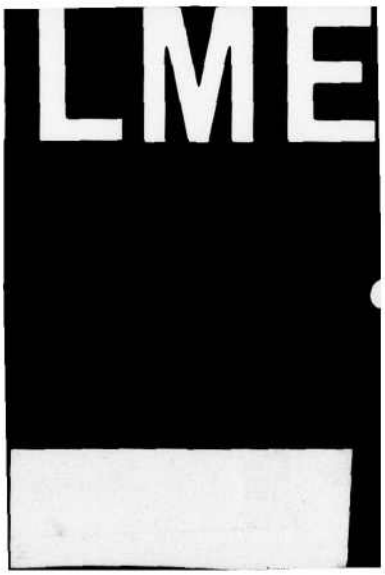
LME